

# Energy-Efficient 5G Outdoor-to-Indoor Communication: SUDAS Over Licensed and Unlicensed Spectrum

Derrick Wing Kwan Ng *Member, IEEE*, Marco Breiling *Member, IEEE*, Christian Rohde, Frank Burkhardt, and Robert Schober *Fellow, IEEE*

**Abstract**—In this paper, we study the design of the user selection, the time allocation to uplink and downlink, and the transceiver processing matrix for uplink and downlink multicarrier transmission employing a shared user equipment (UE)-side distributed antenna system (SUDAS). The proposed SUDAS simultaneously utilizes licensed frequency bands and unlicensed frequency bands with large available bandwidths (e.g. the millimeter wave bands) to enable a spatial multiplexing gain for single-antenna UEs to improve the energy efficiency and throughput of 5-th generation (5G) outdoor-to-indoor communication. The resource allocation algorithm design is formulated as a non-convex optimization problem for the maximization of the end-to-end system energy efficiency (bits/Joule). The non-convex matrix optimization problem is converted to an equivalent non-convex scalar optimization problem for multiple parallel channels, which is solved by an asymptotically globally optimal iterative algorithm. Besides, we propose a suboptimal algorithm which finds a locally optimal solution of the non-convex optimization problem. Simulation results illustrate that the proposed resource allocation algorithms for SUDAS achieve a significant performance gain in terms of system energy efficiency and spectral efficiency compared to conventional baseline systems by offering multiple parallel data streams for single-antenna UEs.

**Index Terms**—5G outdoor-to-indoor communication, OFDMA resource allocation, non-convex optimization.

## I. INTRODUCTION

HIGH data rate, high energy efficiency, and ubiquity are basic requirements for 5-th generation (5G) wireless communication systems. A relevant technique for improving the system throughput for given quality-of-service (QoS) requirements is the combination of massive multiple-input multiple-output (MIMO) [1]–[3] and millimeter wave (mmW) communications [4], [5]. In particular, extra degrees of freedom offered by massive MIMO and the large unlicensed bandwidth in the mmW frequency bands facilitate efficient resource allocation. However, state-of-the-art user equipment (UEs) are typically equipped with a small number of receive

antennas which limits the spatial multiplexing gain offered by MIMO to individual UEs. Besides, the high penetration loss of building walls limits the suitability of mmW for outdoor-to-indoor communication scenarios [6], [7]. Nevertheless, most mobile data traffic is consumed indoors [8] and, hence, an effective system architecture for outdoor-to-indoor communication is needed.

Distributed antenna systems (DAS) are a system architecture on the network side and a special form of MIMO. DAS are able to cover the dead spots in wireless networks, extend service coverage, improve spectral efficiency, and mitigate interference [9], [10]. It is expected that DAS will play an important role in 5G communication systems [11]. Specifically, DAS can realize the potential performance gains of MIMO systems by sharing antennas across the different terminals of a communication system to form a virtual MIMO system [12]. Recently, there has been a growing interest in combining orthogonal frequency division multiple access (OFDMA) and DAS to pave the way for the transition of existing communication systems to 5G [13]–[15]. In [13], the authors studied suboptimal resource allocation algorithms for multiuser MIMO-OFDMA systems. In [14], a utility-based low complexity scheduling scheme was proposed for multiuser MIMO-OFDMA systems to strike a balance between system throughput and computational complexity. Optimal subcarrier allocation, power allocation, and bit loading for OFDMA-DAS was investigated in [15]. However, similar to massive MIMO, DAS cannot significantly improve the data rate of individual UEs when the UEs are single-antenna devices. Besides, since [13]–[15] consider either the downlink or the uplink, the obtained results may no longer be applicable when joint optimization of downlink and uplink resource usage is considered. Furthermore, the total system throughput in [13]–[15] is not only limited by the number of antennas equipped at individual UEs but is also constrained by the system bandwidth which is a very scarce resource in licensed frequency bands. In fact, licensed spectrum is usually located at sub-6 GHz frequencies which are suitable for long distance communication. On the contrary, the unlicensed frequency spectrum around 60 GHz offers a large bandwidth of 7 GHz for wireless communications but is only suitable for short distance communication. This suggests that it may be beneficial to simultaneously utilize both licensed and unlicensed frequency bands for high rate communication which constitutes a paradigm shift in system and resource allocation algorithm design due to the

Derrick Wing Kwan Ng is with the School of Electrical Engineering and Telecommunications, The University of New South Wales, Sydney, Australia (email: {w.k.ng}@unsw.edu.au). Robert Schober is with the Institute for Digital Communications, Friedrich-Alexander-University Erlangen-Nürnberg (FAU), Germany (email: {schober}@int.de). Marco Breiling, Christian Rohde, and Frank Burkhardt are with Fraunhofer Institute for Integrated Circuits (IIS), Erlangen, Germany (email: {marco.breiling, christian.rohde, frank.burkhardt}@iis.fraunhofer.de). This paper has been presented in part at the 81-st IEEE Vehicular Technology Conference, Glasgow, Scotland, May 2015 [1]. This work was supported in part by the AvH Professorship Program of the Alexander von Humboldt Foundation.

related new challenges and opportunities. Yet, the potential system throughput gains of such hybrid systems have not been thoroughly investigated in the literature. Thus, in this work, we study the resource allocation design for hybrid communication systems simultaneously utilizing licensed and unlicensed frequency bands to improve the system performance.

An important requirement for 5G systems is energy efficiency. Over the past decades, the development of wireless communication networks worldwide has triggered an exponential growth in the number of wireless communication devices for real time video teleconferencing, online high definition video streaming, environmental monitoring, and safety management. It is expected that by 2020, the number of interconnected devices on the planet may reach up to 50 billion [16]. The related tremendous increase in the number of wireless transmitters and receivers has not only led to a huge demand for licensed bandwidth but also for energy. In particular, the escalating energy consumption of electronic circuitries for communication and radio frequency (RF) transmission increases the operation cost of service providers and raises serious environmental concerns due to the produced green house gases. As a result, energy efficiency has become as important as spectral efficiency for the evaluation of the performance of the resource utilization in communication networks. As a consequence, a tremendous number of green resource allocation algorithm designs have been proposed in the literature for maximization of the energy efficiency of wireless communication systems [3], [17]–[19]. In [3], joint power allocation and subcarrier allocation was considered for energy-efficient massive MIMO systems. In [17], the energy efficiency of a three-node multiuser MIMO system was studied for the two-hop compress-and-forward relaying protocol. The trade-off between energy efficiency and spectral efficiency in DAS for fair resource allocation in flat fading channels was studied in [18]. Power allocation for energy-efficient DAS was investigated in [19] for frequency-selective channels. However, in [3], [17]–[19], it was assumed that the transmit antennas were deployed by service providers and were connected to a central unit by high cost optical fiber or cable links for facilitating simultaneous transmission which may not be feasible in practice. To avoid this problem, unlicensed and licensed frequency bands may be used simultaneously to create a *wireless data pipeline* for DAS to provide high rate communication services. Nevertheless, the resource allocation algorithm design for such a system architecture has not been investigated in the literature, yet.

In this paper, we address the above issues and the contributions of the paper are summarized as follows:

- We propose a shared UE-side distributed antenna system (SUDAS) to assist the outdoor-to-indoor communication in 5G wireless communication systems. In particular, SUDAS simultaneously utilizes licensed and unlicensed frequency bands to facilitate a spatial multiplexing gain for single-antenna transceivers.
- We formulate the resource allocation algorithm design for SUDAS assisted OFDMA downlink/uplink transmission systems as a non-convex optimization problem. By exploiting the structure of the optimal precoding and post-processing matrices adopted at the BS and the

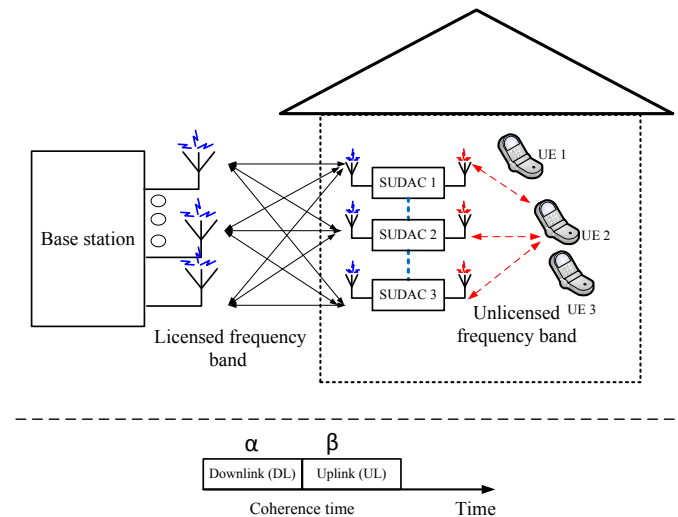


Fig. 1. The upper half of the figure illustrates the downlink and uplink communication between a base station (BS) and  $K = 3$  user equipments (UEs) assisted by  $M = 3$  SUDACs. The proposed system utilizes a licensed frequency band and an unlicensed frequency band such as the mmW band (e.g.  $\sim 60$  GHz). The lower half of the figure depicts the time division duplex (TDD) approach adopted for downlink and uplink communication within a coherence time slot.

SUDAS, the considered matrix optimization problem is transformed into an equivalent optimization problem with scalar optimization variables.

- An iterative algorithm is proposed to achieve the globally optimal performance of the SUDAS asymptotically for high signal-to-noise ratios (SNRs) and large numbers of subcarriers.
- A suboptimal resource allocation algorithm is developed based on the asymptotically optimal algorithm which achieves a locally optimal solution for the considered problem for arbitrary SNRs.

## II. SUDAS ASSISTED OFDMA NETWORK MODEL

### A. SUDAS System Model

We consider a SUDAS assisted OFDMA downlink (DL) and uplink (UL) transmission network which consists of one  $N$  antenna BS, a SUDAS, and  $K$  single-antenna UEs, cf. Figure 1. The BS is half-duplex and equipped with  $N$  antennas for transmitting and receiving signals in a licensed frequency band. The UEs are single-antenna devices receiving and transmitting signals in the unlicensed frequency band. Also, we focus on a wideband multicarrier communication system with  $n_F$  orthogonal subcarriers. The SUDAS comprises  $M$  shared UE-side distributed antenna components (SUDACs). A SUDAC is a small and cheap device deployed inside a building<sup>1</sup> which simultaneously utilizes both a licensed and an unlicensed frequency band for increasing the DL and UL end-to-end communication data rate. A basic SUDAC is equipped with one antenna for use in a licensed band and one antenna for

<sup>1</sup>We note that the SUDAS is designed for assisting outdoor-to-indoor communication. The SUDACs could be integrated into electrical devices such as electrical wall outlets, switches, and light outlets.

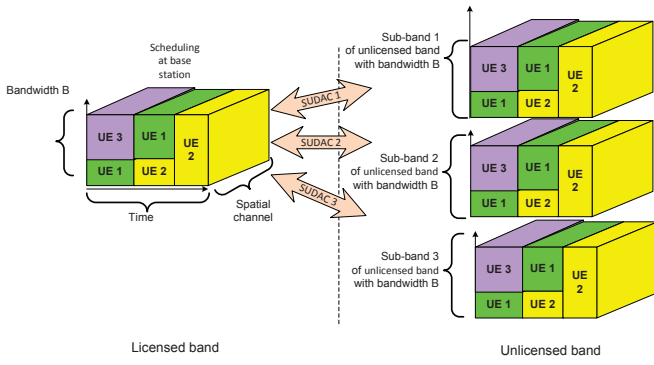


Fig. 2. Illustration of signal forwarding from/(to) a licensed band to/(from) different unlicensed frequency sub-bands in the SUDAS.

use in an unlicensed band. We note that the considered single-antenna model for SUDAC can be extended to the case of antenna arrays at the expense of a higher complexity and a more involved notation. Furthermore, a SUDAC is equipped with a mixer to perform frequency up-conversion/down-conversion. For example, for DL communication, the SUDAC receives the signal from the BS in a licensed frequency band, e.g. at 800 MHz, processes the received signal, and forwards the signal to the UEs in an unlicensed frequency band, e.g. the mmW bands. We note that since the BS-SUDAC link operates in a sub-6 GHz licensed frequency band, it is expected that the associated path loss due to blockage by building walls is much smaller compared to the case where mmW bands are directly used for outdoor-to-indoor communication. Hence, the BS-to-SUDAS channel serves as wireless data pipeline for the SUDAS-to-UE communication channel. Also, since signal reception and transmission at each SUDAC are separated in frequency, cf. Figure 2 and [20], simultaneous signal reception and transmission can be performed in the proposed SUDAS which is not possible for traditional relaying systems<sup>2</sup> due to the limited availability of spectrum in the licensed bands. The UL transmission via SUDAS can be performed in a similar manner as the DL transmission and the detailed operation will be discussed in the next section. In practice, a huge bandwidth is available in the unlicensed bands. For instance, there is nearly 7 GHz of unlicensed frequency spectrum available for information transmission in the 57 – 64 GHz band (mmW band). In this paper, we study the potential system performance gains for outdoor-to-indoor transmission achieved by the proposed SUDAS architecture. In particular, we focus on the case where the SUDACs are installed in electrical wall outlets indoor and can cooperate with each other by sharing channel state information, power, and received signals, e.g.

<sup>2</sup>Since the BS-to-SUDAS and SUDAS-to-UE links operate in two different frequency bands, the proposed SUDAS should not be considered a traditional relaying system [21].

via power line communication links<sup>3</sup>. In other words, for the proposed resource allocation algorithm, joint processing across the SUDACs is assumed to be possible such that the SUDACs can fully exploit the degrees of freedom offered by their antennas. Hence, the joint processing architecture of the SUDAS in this paper reveals the maximum potential performance gain of the proposed SUDAS.

Furthermore, we adopt time division duplexing (TDD) to facilitate UL and DL communication for half-duplex UEs and BS. To simplify the following presentation, we assume a normalized unit length time slot whose duration is the coherence time of the channel, i.e., the communication channel is time-invariant within a time slot. Each time slot is divided into two intervals of duration  $\alpha$  and  $\beta$ , which are allocated for the DL and UL communication, respectively.

*Remark 1:* We note that a SUDAC can perform amplify-and-forward (AF) relaying or compress-and-forward (CF) relaying to facilitate the transmission or reception of multiple data streams. In this paper, we focus on the resource allocation algorithm design for AF SUDACs due to their potentially lower cost in implementation compared to CF SUDACs. We refer to [23] for more details regarding the hardware implementation of SUDACs.

### B. SUDAS DL Channel Model

In the DL transmission period  $\alpha$ , the BS performs *spatial multiplexing* in the licensed band. The data symbol vector  $\mathbf{d}_{\text{DL}}^{[i,k]} \in \mathbb{C}^{N_s \times 1}$  on subcarrier  $i \in \{1, \dots, n_F\}$  for UE  $k \in \{1, \dots, K\}$  is precoded at the BS as

$$\mathbf{x}_{\text{DL}}^{[i,k]} = \mathbf{P}_{\text{DL}}^{[i,k]} \mathbf{d}_{\text{DL}}^{[i,k]}, \quad (1)$$

where  $\mathbf{P}_{\text{DL}}^{[i,k]} \in \mathbb{C}^{N \times N_s}$  is the precoding matrix adopted by the BS on subcarrier  $i$  and  $\mathbb{C}^{N \times N_s}$  denotes the set of all  $N \times N_s$  matrices with complex entries. The signals received on subcarrier  $i$  at the  $M$  SUDACs for UE  $k$  are given by

$$\mathbf{y}_{\text{S-DL}}^{[i,k]} = \mathbf{H}_{\text{B} \rightarrow \text{S}}^{[i]} \mathbf{x}_{\text{DL}}^{[i,k]} + \mathbf{z}^{[i]}, \quad (2)$$

where  $\mathbf{y}_{\text{S-DL}}^{[i,k]} = [y_{\text{S-DL}_1}^{[i,k]}, \dots, y_{\text{S-DL}_M}^{[i,k]}]^T$ ,  $y_{\text{S-DL}_m}^{[i,k]}$  denotes the received signal at SUDAC  $m \in \{1, \dots, M\}$ , and  $(\cdot)^T$  is the transpose operation.  $\mathbf{H}_{\text{B} \rightarrow \text{S}}^{[i]}$  is the  $M \times N$  MIMO channel matrix between the BS and the  $M$  SUDACs on subcarrier  $i$  and captures the joint effects of path loss, shadowing, and multipath fading.  $\mathbf{z}^{[i]}$  is the additive white Gaussian noise (AWGN) vector impairing the  $M$  SUDACs in the licensed band on subcarrier  $i$  and has a circularly symmetric complex Gaussian (CSCG) distribution  $\mathcal{CN}(\mathbf{0}, \mathbf{\Sigma})$  on subcarrier  $i$ , where  $\mathbf{0}$  is the mean vector and  $\mathbf{\Sigma}$  is the  $M \times M$  covariance matrix which is a diagonal matrix with each main diagonal element given by  $N_0$ .

<sup>3</sup>In practice, the backhaul communication between SUDACs can be implemented by optical fibers or power line communication. In fact, the proposed framework can be extended to include the effects of limited backhaul capacity between the SUDACs by following a similar approach as in [22]. However, the main focus of this paper is the introduction of the SUDAS concept and the study of its potential for energy-efficient communication. Thus, the investigation of the impact of a limited backhaul on SUDAS is left for future work.

In the unlicensed band, each SUDAC performs orthogonal *frequency repetition*. In particular, the  $M$  SUDACs multiply the received signal vector on subcarrier  $i$ ,  $\mathbf{y}_{S \rightarrow DL}^{[i,k]}$ , by  $\mathbf{F}_{DL}^{[i,k]} \in \mathbb{C}^{M \times M}$  and forward the processed signal vector to UE  $k$  on subcarrier  $i$  in  $M$  different independent frequency sub-bands in the unlicensed spectrum<sup>4</sup>, cf. Figure 2. In other words, different SUDACs forward their received signals in different sub-bands and thereby avoid multiple access interference in the unlicensed spectrum.

The signal received at UE  $k$  on subcarrier  $i$  from the SUDACs<sup>5</sup> in the  $M$  frequency bands,  $\mathbf{y}_{S \rightarrow UE}^{[i,k]} \in \mathbb{C}^{M \times 1}$ , can be expressed as

$$\begin{aligned} \mathbf{y}_{S \rightarrow UE}^{[i,k]} &= \underbrace{\mathbf{H}_{S \rightarrow UE}^{[i,k]} \mathbf{F}_{DL}^{[i,k]} \mathbf{H}_{B \rightarrow S}^{[i]} \mathbf{P}_{DL}^{[i,k]} \mathbf{d}_{DL}^{[i,k]}}_{\text{desired signal}} \\ &+ \underbrace{\mathbf{H}_{S \rightarrow UE}^{[i,k]} \mathbf{F}_{DL}^{[i,k]} \mathbf{z}^{[i]}}_{\text{amplified noise}} + \mathbf{n}^{[i,k]}. \end{aligned} \quad (3)$$

The  $m$ -th element of vector  $\mathbf{y}_{S \rightarrow UE}^{[i,k]}$  represents the received DL signal at UE  $k$  in the  $m$ -th unlicensed frequency sub-band. Since the SUDACs forward the DL received signals in different orthogonal frequency bands,  $\mathbf{H}_{S \rightarrow UE}^{[i,k]}$  is a diagonal matrix with the diagonal elements representing the channel gains between the SUDACs and UE  $k$  on subcarrier  $i$  in unlicensed sub-band  $m$ .  $\mathbf{n}^{[i,k]} \in \mathbb{C}^{M \times 1}$  is the AWGN vector at UE  $k$  on subcarrier  $i$  with distribution  $\mathcal{CN}(\mathbf{0}, \mathbf{\Sigma}_k)$ , where  $\mathbf{\Sigma}_k$  is an  $M \times M$  diagonal matrix and each main diagonal element is equal to  $N_{UE_k}$ .

We assume that  $M \geq N_S$  and UE  $k$  employs a linear receiver for estimating the DL data vector symbol received in the  $M$  different sub-bands in the unlicensed band. Hence, the estimated data vector symbol,  $\hat{\mathbf{d}}_{DL}^{[i,k]} \in \mathbb{C}^{N_S \times 1}$ , on subcarrier  $i$  at UE  $k$  is given by

$$\hat{\mathbf{d}}_{DL}^{[i,k]} = (\mathbf{W}_{DL}^{[i,k]})^H \mathbf{y}_{S \rightarrow UE}^{[i,k]}, \quad (4)$$

where  $\mathbf{W}_{DL}^{[i,k]} \in \mathbb{C}^{M \times N_S}$  is a post-processing matrix applied in subcarrier  $i$  at UE  $k$ , and  $(\cdot)^H$  denotes the Hermitian transpose. Without loss of generality, we assume that  $\mathcal{E}\{\mathbf{d}_{DL}^{[i,k]} (\mathbf{d}_{DL}^{[i,k]})^H\} = \mathbf{I}_{N_S}$  where  $\mathbf{I}_{N_S}$  is an  $N_S \times N_S$  identity matrix and  $\mathcal{E}\{\cdot\}$  denotes statistical expectation. In other words, for each antenna, the power of the downlink symbols in the baseband is normalized to one, which is a commonly adopted normalization in the literature for precoder design [24], [25]. The minimum mean square error (MMSE) matrix for data transmission on subcarrier  $i$  for UE  $k$  via the proposed SUDAS and the optimal MMSE post-processing matrix are given by

$$\begin{aligned} \mathbf{E}_{DL}^{[i,k]} &= \mathcal{E}\{(\hat{\mathbf{d}}_{DL}^{[i,k]} - \mathbf{d}_{DL}^{[i,k]})(\hat{\mathbf{d}}_{DL}^{[i,k]} - \mathbf{d}_{DL}^{[i,k]})^H\} \\ &= \left[ \mathbf{I}_{N_S} + (\mathbf{\Gamma}_{DL}^{[i,k]})^H (\mathbf{\Theta}_{DL}^{[i,k]})^{-1} \mathbf{\Gamma}_{DL}^{[i,k]} \right]^{-1}, \end{aligned} \quad (5)$$

$$\text{and } \mathbf{W}_{DL}^{[i,k]} = (\mathbf{\Gamma}_{DL}^{[i,k]} (\mathbf{\Gamma}_{DL}^{[i,k]})^H + \mathbf{\Theta}_{DL}^{[i,k]})^{-1} \mathbf{\Gamma}_{DL}^{[i,k]}, \quad (6)$$

<sup>4</sup>For a signal bandwidth of 20 MHz, there are 350 orthogonal sub-bands available within 7 GHz of bandwidth in the 60 GHz mmW band [5]. For simplicity, we assume that each of the  $M$  SUDACs uses one fixed sub-band for DL and UL communication.

<sup>5</sup>We note that the signal model considered in the paper can be easily extended such that the indoor UEs can use both the licensed and the unlicensed bands for communication.

respectively, where  $(\cdot)^{-1}$  denotes the matrix inverse,  $\mathbf{\Gamma}_{DL}^{[i,k]}$  is the effective end-to-end channel matrix from the BS to UE  $k$  via the SUDAS on subcarrier  $i$ , and  $\mathbf{\Theta}_{DL}^{[i,k]}$  is the corresponding equivalent noise covariance matrix. These matrices are given by

$$\begin{aligned} \mathbf{\Gamma}_{DL}^{[i,k]} &= \mathbf{H}_{S \rightarrow UE}^{[i,k]} \mathbf{F}_{DL}^{[i,k]} \mathbf{H}_{B \rightarrow S}^{[i]} \mathbf{P}_{DL}^{[i,k]} \quad \text{and} \\ \mathbf{\Theta}_{DL}^{[i,k]} &= \left( \mathbf{H}_{S \rightarrow UE}^{[i,k]} \mathbf{F}_{DL}^{[i,k]} \right) \left( \mathbf{H}_{S \rightarrow UE}^{[i,k]} \mathbf{F}_{DL}^{[i,k]} \right)^H + \mathbf{I}_M. \end{aligned} \quad (7)$$

### C. SUDAS UL Channel Model

In the UL transmission period  $\beta$ , UE  $k$  performs *frequency multiplexing* in the unlicensed band. The data symbol vector  $\mathbf{d}_{UL}^{[i,k]} \in \mathbb{C}^{N_S \times 1}$  on subcarrier  $i \in \{1, \dots, n_F\}$  from UE  $k$  is precoded as

$$\mathbf{x}_{UL}^{[i,k]} = \mathbf{P}_{UL}^{[i,k]} \mathbf{d}_{UL}^{[i,k]}, \quad (8)$$

where  $\mathbf{P}_{UL}^{[i,k]} \in \mathbb{C}^{M \times N_S}$  is the UL precoding matrix adopted by UE  $k$  on subcarrier  $i$  over the  $M$  different frequency sub-bands in the unlicensed spectrum. The signals received on subcarrier  $i$  at the  $M$  SUDACs for UE  $k$  are given by

$$\mathbf{y}_{S \rightarrow UL}^{[i,k]} = \mathbf{H}_{UE \rightarrow S}^{[i,k]} \mathbf{x}_{UL}^{[i,k]} + \mathbf{v}^{[i]}, \quad (9)$$

where  $\mathbf{y}_{S \rightarrow UL}^{[i,k]} = [y_{S \rightarrow UL_1}^{[i,k]} \dots y_{S \rightarrow UL_M}^{[i,k]}]^T$ ,  $y_{S \rightarrow UL_m}^{[i,k]}$  denotes the received signal at SUDAC  $m$  in unlicensed frequency sub-band  $m \in \{1, \dots, M\}$ , and  $\mathbf{v}^{[i]}$  is the AWGN impairing the  $M$  SUDACs on subcarrier  $i$  in the unlicensed frequency band.  $\mathbf{v}^{[i]}$  has distribution  $\mathcal{CN}(\mathbf{0}, \mathbf{\Sigma}_{UL})$ , where  $\mathbf{\Sigma}_{UL}$  is an  $M \times M$  diagonal matrix and each main diagonal element is equal to  $N_{UL}$ .  $\mathbf{H}_{UE \rightarrow S}^{[i,k]}$  is a diagonal matrix with the main diagonal elements representing the channel gains between UE  $k$  and the  $M$  SUDACs on subcarrier  $i$  in unlicensed sub-band  $m$ . In fact, the UEs-to-SUDAS channels serve as a short distance wireless data pipeline for the SUDAS-to-BS UL communication.

Each SUDAC forwards the signals received in the unlicensed band in the licensed band to assist the UL communication. In particular, the  $M$  SUDACs multiply the received signal vector on subcarrier  $i$  by  $\mathbf{F}_{UL}^{[i,k]} \in \mathbb{C}^{M \times M}$  and forward the processed signal vector to the BS on subcarrier  $i$  in the licensed spectrum, cf. Figure 2. As a result, the signal received at the BS from UE  $k$  on subcarrier  $i$  via the SUDAS,  $\mathbf{y}_{S \rightarrow B}^{[i,k]} \in \mathbb{C}^{N \times 1}$ , can be expressed as

$$\begin{aligned} \mathbf{y}_{S \rightarrow B}^{[i,k]} &= \underbrace{\mathbf{H}_{S \rightarrow B}^{[i]} \mathbf{F}_{UL}^{[i,k]} \mathbf{H}_{UE \rightarrow S}^{[i,k]} \mathbf{P}_{UL}^{[i,k]} \mathbf{d}_{UL}^{[i,k]}}_{\text{desired signal}} \\ &+ \underbrace{\mathbf{H}_{S \rightarrow B}^{[i]} \mathbf{F}_{UL}^{[i,k]} \mathbf{z}^{[i]}}_{\text{amplified noise}} + \mathbf{n}_B^{[i,k]}. \end{aligned} \quad (10)$$

Matrix  $\mathbf{H}_{S \rightarrow B}^{[i]}$  is the UL channel between the  $M$  SUDACs and the BS on subcarrier  $i$ , and  $\mathbf{n}_B^{[i,k]}$  is the AWGN vector in subcarrier  $i$  at the BS with distribution  $\mathcal{CN}(\mathbf{0}, \mathbf{\Sigma}_B)$ , where  $\mathbf{\Sigma}_B$  is an  $M \times M$  diagonal matrix and each main diagonal element is equal to  $N_B$ . At the BS, we assume that  $N \geq N_S$  and the BS employs a linear receiver for estimating the data vector symbol received from the SUDAS in the licensed band. The

estimated data vector symbol,  $\hat{\mathbf{d}}_{\text{UL}}^{[i,k]} \in \mathbb{C}^{N_s \times 1}$ , on subcarrier  $i$  at the BS from UE  $k$  is given by

$$\hat{\mathbf{d}}_{\text{UL}}^{[i,k]} = (\mathbf{W}_{\text{UL}}^{[i,k]})^H \mathbf{y}_{\text{S} \rightarrow \text{B}}^{[i,k]}, \quad (11)$$

where  $\mathbf{W}_{\text{UL}}^{[i,k]} \in \mathbb{C}^{M \times N_s}$  is a post-processing matrix used for subcarrier  $i$  at UE  $k$ . Without loss of generality, we assume for the uplink data vector signal the same normalization as for the downlink data vector signal, i.e.,  $\mathcal{E}\{\mathbf{d}_{\text{UL}}^{[i,k]}(\mathbf{d}_{\text{UL}}^{[i,k]})^H\} = \mathbf{I}_{N_s}$ . As a result, the MMSE matrix for data transmission on subcarrier  $i$  from UE  $k$  to the BS via the SUDAS and the optimal MMSE post-processing matrix are given by

$$\mathbf{E}_{\text{UL}}^{[i,k]} = \mathcal{E}\{(\hat{\mathbf{d}}_{\text{UL}}^{[i,k]} - \mathbf{d}_{\text{UL}}^{[i,k]})(\hat{\mathbf{d}}_{\text{UL}}^{[i,k]} - \mathbf{d}_{\text{UL}}^{[i,k]})^H\} \\ = \left[ \mathbf{I}_{N_s} + (\mathbf{\Gamma}_{\text{UL}}^{[i,k]})^H (\mathbf{\Theta}_{\text{UL}}^{[i,k]})^{-1} \mathbf{\Gamma}_{\text{UL}}^{[i,k]} \right]^{-1}, \quad (12)$$

$$\text{and } \mathbf{W}_{\text{UL}}^{[i,k]} = (\mathbf{\Gamma}_{\text{UL}}^{[i,k]} (\mathbf{\Gamma}_{\text{UL}}^{[i,k]})^H + \mathbf{\Theta}_{\text{UL}}^{[i,k]})^{-1} \mathbf{\Gamma}_{\text{UL}}^{[i,k]}, \quad (13)$$

respectively, where  $\mathbf{\Gamma}_{\text{UL}}^{[i,k]}$  is the effective end-to-end channel matrix from UE  $k$  to the BS via the SUDAS on subcarrier  $i$ , and  $\mathbf{\Theta}_{\text{UL}}^{[i,k]}$  is the corresponding equivalent noise covariance matrix. These matrices are given by

$$\mathbf{\Gamma}_{\text{UL}}^{[i,k]} = \mathbf{H}_{\text{S} \rightarrow \text{B}}^{[i]} \mathbf{F}_{\text{UL}}^{[i,k]} \mathbf{H}_{\text{UE} \rightarrow \text{S}}^{[i,k]} \mathbf{P}_{\text{UL}}^{[i,k]} \quad \text{and} \\ \mathbf{\Theta}_{\text{UL}}^{[i,k]} = \left( \mathbf{H}_{\text{UE} \rightarrow \text{S}}^{[i,k]} \mathbf{F}_{\text{UL}}^{[i,k]} \right) \left( \mathbf{H}_{\text{UE} \rightarrow \text{S}}^{[i,k]} \mathbf{F}_{\text{UL}}^{[i,k]} \right)^H + \mathbf{I}_M. \quad (14)$$

*Remark 2:* Since TDD is adopted and DL and UL transmission occur consecutively within the same coherence time, for resource allocation algorithm design, it is reasonable to assume that channel reciprocity holds, i.e.,  $\mathbf{H}_{\text{UE} \rightarrow \text{S}}^{[i,k]} = (\mathbf{H}_{\text{S} \rightarrow \text{UE}}^{[i,k]})^H$  and  $\mathbf{H}_{\text{S} \rightarrow \text{B}}^{[i]} = (\mathbf{H}_{\text{B} \rightarrow \text{S}}^{[i]})^H$ .

*Remark 3:* We note that existing systems such as LTE-A enable both in-band and out-of-band relaying which, at first glance, has a similar architecture as the proposed SUDAS. However, both types of relaying in LTE-A take place in licensed bands. Besides, the functionality and application scenarios of SUDAS are different from those of traditional relaying systems in the literature which aim at extending service coverage [26], [27]. Traditional relays are usually deployed by service providers and installed at fixed locations. In contrast, the proposed SUDAS is deployed by the end users indoor and not at a priori fixed locations. On the other hand, licensed spectrum is usually located at sub-6 GHz frequencies which are suitable for long distance communication but have limited bandwidth available. In contrast, the unlicensed frequency spectrum around 60 GHz offers a large bandwidth of 7 GHz for wireless communications but is limited to short distance communication. In fact, the characteristics of the licensed and the unlicensed bands complement each other. The proposed SUDAS acts as a bridge to connect two bands to facilitate the conversion of spatial multiplexing gains and frequency multiplexing gains such that single-antenna UEs are able to transmit/receive multiple parallel data streams on each subcarrier.

### III. PROBLEM FORMULATION

In this section, we first introduce the adopted system performance measure. Then, the design of resource allocation and scheduling is formulated as an optimization problem.

#### A. System Throughput, Power Consumption, and Energy Efficiency

The end-to-end DL and UL achievable data rates on subcarrier  $i$  between the BS and UE  $k$  via the SUDAS are given by [24]

$$R_{\text{DL}}^{[i,k]} = -\log_2 \left( \det[\mathbf{E}_{\text{DL}}^{[i,k]}] \right) \quad \text{and} \\ R_{\text{UL}}^{[i,k]} = -\log_2 \left( \det[\mathbf{E}_{\text{UL}}^{[i,k]}] \right), \quad (15)$$

respectively, where  $\det(\cdot)$  is the determinant operation. The DL and UL data rates (bits/s) for UE  $k$  can be expressed as

$$\rho_{\text{DL}}^{[k]} = \sum_{i=1}^{n_F} s_{\text{DL}}^{[i,k]} R_{\text{UL}}^{[i,k]} \quad \text{and} \quad \rho_{\text{UL}}^{[k]} = \sum_{i=1}^{n_F} s_{\text{UL}}^{[i,k]} R_{\text{DL}}^{[i,k]}, \quad (16)$$

respectively, where  $s_{\text{DL}}^{[i,k]} \in \{0, \alpha\}$  and  $s_{\text{UL}}^{[i,k]} \in \{0, \beta\}$  are the discrete subcarrier allocation indicators, respectively. In particular, a DL and an UL subcarrier can only be utilized for  $\alpha$  and  $\beta$  portions of the coherence time, respectively, or not be used at all.

The system throughput is given by

$$\mathcal{U}(\mathcal{P}, \mathcal{S}) = \sum_{k=1}^K \rho_{\text{DL}}^{[k]} + \sum_{k=1}^K \rho_{\text{UL}}^{[k]} \quad [\text{bits/s}], \quad (17)$$

where  $\mathcal{P} = \{\mathbf{P}_{\text{DL}}^{[i,k]}, \mathbf{F}_{\text{DL}}^{[i,k]}, \mathbf{P}_{\text{UL}}^{[i,k]}, \mathbf{F}_{\text{UL}}^{[i,k]}\}$  and  $\mathcal{S} = \{s_{\text{DL}}^{[i,k]}, s_{\text{UL}}^{[i,k]}, \alpha, \beta\}$  are the precoding and subcarrier allocation policies, respectively.

On the other hand, the power consumption of the considered SUDAS assisted communication system (Joule/s) consists of seven terms which can be divided into three groups and expressed as

$$\mathcal{U}_{\text{TP}}(\mathcal{P}, \mathcal{S}) \\ = \underbrace{P_{\text{CB}} + NP_{\text{AntB}} + MP_{\text{CSUDAC}} + KP_{\text{CUE}}}_{\text{System circuit power consumption}} \quad (18a)$$

$$+ \underbrace{\sum_{k=1}^K \sum_{i=1}^{n_F} s_{\text{DL}}^{[i,k]} \varepsilon_{\text{B}} \text{Tr}(\mathbf{\Phi}_{\text{DL}}^{[i,k]}) + s_{\text{DL}}^{[i,k]} \varepsilon_{\text{S}} \text{Tr}(\mathbf{G}_{\text{DL}}^{[i,k]})}_{\text{Total DL transmit power consumption}} \quad (18b)$$

$$+ \underbrace{\sum_{k=1}^K \sum_{i=1}^{n_F} \varepsilon_k s_{\text{UL}}^{[i,k]} \text{Tr}(\mathbf{\Phi}_{\text{UL}}^{[i,k]}) + s_{\text{UL}}^{[i,k]} \varepsilon_{\text{S}} \text{Tr}(\mathbf{G}_{\text{UL}}^{[i,k]})}_{\text{Total UL transmit power consumption}} \quad (18c)$$

where

$$\mathbf{\Phi}_{\text{UL}}^{[i,k]} = \mathbf{P}_{\text{UL}}^{[i,k]} (\mathbf{P}_{\text{UL}}^{[i,k]})^H \quad (19)$$

$$\mathbf{\Phi}_{\text{DL}}^{[i,k]} = \mathbf{P}_{\text{DL}}^{[i,k]} (\mathbf{P}_{\text{DL}}^{[i,k]})^H \quad (20)$$

$$\mathbf{G}_{\text{DL}}^{[i,k]} = \mathbf{F}_{\text{DL}}^{[i,k]} \left( \mathbf{H}_{\text{B} \rightarrow \text{S}}^{[i]} \mathbf{\Phi}_{\text{DL}}^{[i,k]} (\mathbf{H}_{\text{B} \rightarrow \text{S}}^{[i]})^H + \mathbf{I}_M \right) (\mathbf{F}_{\text{DL}}^{[i,k]})^H, \quad (21)$$

$$\mathbf{G}_{\text{UL}}^{[i,k]} = \mathbf{F}_{\text{UL}}^{[i,k]} \left( \mathbf{H}_{\text{UE} \rightarrow \text{S}}^{[i,k]} \mathbf{\Phi}_{\text{UL}}^{[i,k]} (\mathbf{H}_{\text{UE} \rightarrow \text{S}}^{[i,k]})^H + \mathbf{I}_M \right) (\mathbf{F}_{\text{UL}}^{[i,k]})^H, \quad (22)$$

and  $\text{Tr}(\cdot)$  is the trace operator. The three positive constant terms in (18a), i.e.,  $P_{\text{CB}}$ ,  $P_{\text{CSUDAC}}$ , and  $P_{\text{CUE}}$ , represent the power dissipation of the circuits [22] for the basic operation of the BS, the SUDAC, and the UE, respectively, and  $P_{\text{AntB}}$

denotes the circuit power consumption per BS antenna. Equations (18b) and (18c) denote the total DL and the total UL transmit power consumptions, respectively. Specifically,  $\text{Tr}(\mathbf{G}_{\text{DL}}^{[i,k]})$  and  $\text{Tr}(\mathbf{G}_{\text{UL}}^{[i,k]})$  are the DL and UL transmit powers of the SUDAS needed for facilitating the DL and UL communication of UE  $k$  in subcarrier  $i$ , respectively. Similarly,  $\text{Tr}(\mathbf{P}_{\text{DL}}^{[i,k]}(\mathbf{P}_{\text{DL}}^{[i,k]})^H)$  and  $\text{Tr}(\mathbf{P}_{\text{UL}}^{[i,k]}(\mathbf{P}_{\text{UL}}^{[i,k]})^H)$  represent the DL transmit power from the BS to the SUDAS for UE  $k$  and the UL transmit power from UE  $k$  to the SUDAS in subcarrier  $i$ , respectively. To capture the power inefficiency of the power amplifiers, we introduce in (18) linear multiplicative constants  $\varepsilon_B$ ,  $\varepsilon_S$ , and  $\varepsilon_k$  for the power radiated by the BS, the SUDAS, and UE  $k$ , respectively. For instance, if  $\varepsilon_B = 4$ , then for 1 Watt of power radiated in the RF, the BS consumes 4 Watt of power which leads to a power amplifier efficiency of 25%<sup>6</sup>.

The *energy efficiency* of the considered system is defined as the total number of bits exchanged between the BS and the  $K$  UEs via the SUDAS per Joule consumed energy:

$$U_{\text{eff}}(\mathcal{P}, \mathcal{S}) = \frac{\mathcal{U}(\mathcal{P}, \mathcal{S})}{\mathcal{U}_{\text{TP}}(\mathcal{P}, \mathcal{S})} \quad [\text{bits/Joule}]. \quad (23)$$

### B. Optimization Problem Formulation

The optimal precoding matrices,  $\mathcal{P}^* = \{\mathbf{P}_{\text{DL}}^{[i,k]*}, \mathbf{F}_{\text{DL}}^{[i,k]*}, \mathbf{P}_{\text{UL}}^{[i,k]*}, \mathbf{F}_{\text{UL}}^{[i,k]*}\}$ , and the optimal subcarrier allocation policy,  $\mathcal{S}^* = \{s_{\text{DL}}^{[i,k]*}, s_{\text{UL}}^{[i,k]*}, \alpha^*, \beta^*\}$ , can be obtained by solving the following optimization problem:

$$\begin{aligned} & \underset{\mathcal{P}, \mathcal{S}}{\text{maximize}} \quad U_{\text{eff}}(\mathcal{P}, \mathcal{S}) \\ \text{s.t.} \quad & \text{C1: } \sum_{k=1}^K \sum_{i=1}^{n_F} s_{\text{DL}}^{[i,k]} \text{Tr}(\mathbf{P}_{\text{DL}}^{[i,k]}(\mathbf{P}_{\text{DL}}^{[i,k]})^H) \leq P_T, \\ & \text{C2: } \sum_{k=1}^K \sum_{i=1}^{n_F} s_{\text{DL}}^{[i,k]} \text{Tr}(\mathbf{G}_{\text{DL}}^{[i,k]}) \leq MP_{\text{max}}, \\ & \text{C3: } \sum_{i=1}^{n_F} s_{\text{UL}}^{[i,k]} \text{Tr}(\mathbf{P}_{\text{UL}}^{[i,k]}(\mathbf{P}_{\text{UL}}^{[i,k]})^H) \leq P_{\text{max}_k}, \forall k, \\ & \text{C4: } \sum_{k=1}^K \sum_{i=1}^{n_F} s_{\text{UL}}^{[i,k]} \text{Tr}(\mathbf{G}_{\text{UL}}^{[i,k]}) \leq P_{\text{max}}^{\text{UL}}, \\ & \text{C5: } \rho_{\text{DL}}^{[k]} \geq R_{\text{min}_k}^{\text{DL}}, \forall k \in \mathcal{D}_{\text{DL}}, \quad \text{C6: } \rho_{\text{UL}}^{[k]} \geq R_{\text{min}_k}^{\text{UL}}, \forall k \in \mathcal{D}_{\text{UL}}, \\ & \text{C7: } \sum_{i=1}^{n_F} s_{\text{DL}}^{[i,k]} \leq \alpha, \forall i, \quad \text{C8: } \sum_{i=1}^{n_F} s_{\text{UL}}^{[i,k]} \leq \beta, \quad \forall i, \\ & \text{C9: } s_{\text{DL}}^{[i,k]} \in \{0, \alpha\}, \forall i, k, \quad \text{C10: } s_{\text{UL}}^{[i,k]} \in \{0, \beta\}, \forall i, k, \\ & \text{C11: } \alpha + \beta \leq 1, \quad \text{C12: } \alpha, \beta \geq 0. \end{aligned} \quad (24)$$

Constants  $P_T$  and  $MP_{\text{max}}$  in C1 and C2 are the maximum transmit power allowances for the BS and the SUDAS ( $M$  SUDACs) for DL transmission, respectively, where  $P_{\text{max}}$  is the average transmit power budget for a SUDAC. Similarly, constraints C3 and C4 limit the transmit power for UE  $k$  and the SUDAS ( $M$  SUDACs) for UL transmission, respectively, where  $P_{\text{max}_k}$  and  $P_{\text{max}}^{\text{UL}}$  are the maximum transmit power

budgets of UE  $k$  and the SUDAS, respectively. We note that in practice the maximum transmit power allowances for the SUDAS-to-UE link,  $P_{\text{max}}$ , and SUDAS-to-BS link,  $P_{\text{max}}^{\text{UL}}$ , may be different due to different regulations in licensed and unlicensed bands. Sets  $\mathcal{D}_{\text{DL}}$  and  $\mathcal{D}_{\text{UL}}$  in constraints C5 and C6 denote the sets of delay sensitive UEs for DL and UL communication, respectively. In particular, the system has to guarantee a minimum required DL data rate  $R_{\text{min}_k}^{\text{DL}}$  and UL data rate  $R_{\text{min}_k}^{\text{UL}}$ , if UE  $k$  requests delay sensitive services in the DL and UL, respectively. Constraints C7–C10 are imposed to guarantee that each subcarrier can serve at most one UE for DL and UL communication for fractions of  $\alpha$  and  $\beta$  of the available time, respectively. Constraints C11 and C12 are the boundary conditions for the durations of DL and UL transmission.

### IV. RESOURCE ALLOCATION ALGORITHM DESIGN

The considered optimization problem has a non-convex objective function in fractional form. Besides, the precoding matrices  $\{\mathbf{P}_{\text{DL}}^{[i,k]}, \mathbf{P}_{\text{UL}}^{[i,k]}\}$  and  $\{\mathbf{F}_{\text{DL}}^{[i,k]}, \mathbf{F}_{\text{UL}}^{[i,k]}\}$  are coupled in (21) and (22) leading to a non-convex feasible solution set in (24). Also, constraints C9 and C10 are combinatorial constraints which results in a discontinuity in the solution set. In general, there is no systematic approach for solving non-convex optimization problems optimally. In many cases, an exhaustive search method may be needed to obtain the global optimal solution. Yet, applying such method to our problem will lead to prohibitively high computational complexity since the search space for the optimal solution grows exponentially with respect to  $K$  and  $n_F$ . In order to make the problem tractable, we first transform the objective function in fractional form into an equivalent objective function in subtractive form via fractional programming theory. Subsequently, majorization theory is exploited to obtain the structure of the optimal precoding policy to further simplify the problem. Then, we employ constraint relaxation to handle the binary constraints C9 and C10 to obtain an asymptotically optimal resource allocation algorithm in the high SNR regime and for large numbers of subcarriers.

#### A. Transformation of the Optimization Problem

For notational simplicity, we define  $\mathcal{F}$  as the set of feasible solutions of the optimization problem in (24) spanned by constraints C1 – C12. Without loss of generality, we assume that  $\{\mathcal{P}, \mathcal{S}\} \in \mathcal{F}$  and the solution set  $\mathcal{F}$  is non-empty and compact. Then, the maximum energy efficiency of the SUDAS assisted communication, denoted as  $\eta_{\text{eff}}^*$ , is given by

$$\eta_{\text{eff}}^* = \frac{\mathcal{U}(\mathcal{P}^*, \mathcal{S}^*)}{\mathcal{U}_{\text{TP}}(\mathcal{P}^*, \mathcal{S}^*)} = \underset{\{\mathcal{P}, \mathcal{S}\} \in \mathcal{F}}{\text{maximize}} \frac{\mathcal{U}(\mathcal{P}, \mathcal{S})}{\mathcal{U}_{\text{TP}}(\mathcal{P}, \mathcal{S})}. \quad (25)$$

Now, we introduce the following theorem for handling the optimization problem in (24).

*Theorem 1:* By nonlinear fractional programming theory [28], [29], the resource allocation policy achieves the maximum energy efficiency  $\eta_{\text{eff}}^*$  if and only if it satisfies

$$\begin{aligned} & \underset{\{\mathcal{P}, \mathcal{S}\} \in \mathcal{F}}{\text{maximize}} \quad \mathcal{U}(\mathcal{P}, \mathcal{S}) - \eta_{\text{eff}}^* \mathcal{U}_{\text{TP}}(\mathcal{P}, \mathcal{S}) \\ & = \mathcal{U}(\mathcal{P}^*, \mathcal{S}^*) - \eta_{\text{eff}}^* \mathcal{U}_{\text{TP}}(\mathcal{P}^*, \mathcal{S}^*) = 0, \end{aligned} \quad (26)$$

<sup>6</sup>In this paper, we assume that Class A power amplifiers with linear characteristic are implemented at the transceivers. The maximum power efficiency of Class A amplifiers is limited to 25%.

TABLE I  
ITERATIVE RESOURCE ALLOCATION ALGORITHM.

**Algorithm 1** Iterative Resource Allocation Algorithm

---

1: Initialization:  $N_{\text{Iter}}^{\text{Dinkelbach}}$  the maximum number of iterations and  $\Delta \rightarrow 0$  is the maximum tolerance  
2: Set  $\eta_{\text{eff}} = 0$  and iteration index  $t = 0$   
3: **repeat** {Iteration Process: Main Loop}  
4:   For a given  $\eta_{\text{eff}}$ , solve (27) and obtain an intermediate resource allocation policy  $\{\mathcal{P}', \mathcal{S}'\}$   
5:   **if**  $|\mathcal{U}(\mathcal{P}', \mathcal{S}') - \eta_{\text{eff}} \mathcal{U}_{\text{TP}}(\mathcal{P}', \mathcal{S}')| < \Delta$  **then**  
6:     Convergence = **true**,   **return**  $\{\mathcal{P}^*, \mathcal{S}^*\} = \{\mathcal{P}', \mathcal{S}'\}$  and  $\eta_{\text{eff}}^* = \frac{\mathcal{U}(\mathcal{P}', \mathcal{S}')}{\mathcal{U}_{\text{TP}}(\mathcal{P}', \mathcal{S}')}$   
7:   **else**  
8:     Set  $\eta_{\text{eff}} = \frac{\mathcal{U}(\mathcal{P}', \mathcal{S}')}{\mathcal{U}_{\text{TP}}(\mathcal{P}', \mathcal{S}')}$  and  $t = t + 1$ , convergence = **false**  
9:   **end if**  
10: **until** Convergence = **true** or  $t = N_{\text{Iter}}^{\text{Dinkelbach}}$

---

for  $\mathcal{U}(\mathcal{P}, \mathcal{S}) \geq 0$  and  $\mathcal{U}_{\text{TP}}(\mathcal{P}, \mathcal{S}) > 0$ .

*Proof:* Please refer to [28], [29] for a proof of Theorem 1. ■

Theorem 1 states the necessary and sufficient condition for a resource allocation policy to be globally optimal. Hence, for an optimization problem with an objective function in fractional form, there exists an equivalent optimization problem with an objective function in subtractive form, e.g.  $\mathcal{U}(\mathcal{P}^*, \mathcal{S}^*) - \eta_{\text{eff}}^* \mathcal{U}_{\text{TP}}(\mathcal{P}^*, \mathcal{S}^*)$  in this paper, such that the same optimal resource allocation policy solves both problems. Therefore, without loss of generality, we can focus on the objective function in equivalent subtractive form to design a resource allocation policy which satisfies Theorem 1 in the sequel.

**B. Asymptotically Optimal Solution**

In this section, we propose an asymptotically optimal iterative algorithm based on the Dinkelbach method [28] for solving (24) with an equivalent objective function such that the obtained solution satisfies the conditions stated in Theorem 1. The proposed iterative algorithm is summarized in Table I and the convergence to the optimal energy efficiency is guaranteed if the inner problem (27) is solved in each iteration. Please refer to [28] for a proof of the convergence of the iterative algorithm.

The iterative algorithm is implemented with a repeated loop. In each iteration in the main loop, i.e., lines 3 – 10, we solve the following optimization problem for a given parameter  $\eta_{\text{eff}}$ :

$$\begin{aligned} & \underset{\mathcal{P}, \mathcal{S}}{\text{maximize}} \quad \mathcal{U}(\mathcal{P}, \mathcal{S}) - \eta_{\text{eff}} \mathcal{U}_{\text{TP}}(\mathcal{P}, \mathcal{S}) \\ & \text{s.t.} \quad \text{C1} - \text{C12}. \end{aligned} \quad (27)$$

*Solution of the Main Loop Problem (27):* The transformed objective function is in subtractive form and is parameterized by variable  $\eta_{\text{eff}}$ . Yet, the transformed problem is still a non-convex optimization problem. We handle the coupled precoding matrices by studying the structure of the optimal precoding matrices for (27). In this context, we define the following matrices to facilitate the subsequent presentation.

Using singular value decomposition (SVD), the DL two-hop channel matrices  $\mathbf{H}_{\text{B} \rightarrow \text{S}}^{[i]}$  and  $\mathbf{H}_{\text{S} \rightarrow \text{UE}}^{[i,k]}$  can be written as

$$\begin{aligned} \mathbf{H}_{\text{B} \rightarrow \text{S}}^{[i]} &= \mathbf{U}_{\text{B} \rightarrow \text{S}}^{[i]} \mathbf{\Lambda}_{\text{B} \rightarrow \text{S}}^{[i]} (\mathbf{V}_{\text{B} \rightarrow \text{S}}^{[i]})^H \quad \text{and} \\ \mathbf{H}_{\text{S} \rightarrow \text{UE}}^{[i,k]} &= \mathbf{U}_{\text{S} \rightarrow \text{UE}}^{[i,k]} \mathbf{\Lambda}_{\text{S} \rightarrow \text{UE}}^{[i,k]} (\mathbf{V}_{\text{S} \rightarrow \text{UE}}^{[i,k]})^H, \end{aligned} \quad (28)$$

respectively, where  $\mathbf{U}_{\text{B} \rightarrow \text{S}}^{[i]} \in \mathbb{C}^{M \times M}$ ,  $\mathbf{V}_{\text{B} \rightarrow \text{S}}^{[i]} \in \mathbb{C}^{N \times N}$ ,  $\mathbf{U}_{\text{S} \rightarrow \text{UE}}^{[i,k]} \in \mathbb{C}^{M \times M}$ , and  $\mathbf{V}_{\text{S} \rightarrow \text{UE}}^{[i,k]} \in \mathbb{C}^{M \times M}$  are unitary matrices.  $\mathbf{\Lambda}_{\text{B} \rightarrow \text{S}}^{[i]}$  and  $\mathbf{\Lambda}_{\text{S} \rightarrow \text{UE}}^{[i,k]}$  are  $M \times N$  and  $M \times M$  matrices with main diagonal element vectors  $\left[ \sqrt{\gamma_{\text{B} \rightarrow \text{S},1}^{[i]}} \sqrt{\gamma_{\text{B} \rightarrow \text{S},2}^{[i]}} \cdots \sqrt{\gamma_{\text{B} \rightarrow \text{S},R_1}^{[i]}} \right]$  and  $\left[ \sqrt{\gamma_{\text{S} \rightarrow \text{UE},1}^{[i,k]}} \sqrt{\gamma_{\text{S} \rightarrow \text{UE},2}^{[i,k]}} \cdots \sqrt{\gamma_{\text{S} \rightarrow \text{UE},R_2}^{[i,k]}} \right]$ , respectively, and all other elements equal to zero. Subscript indices  $R_1 = \text{Rank}(\mathbf{H}_{\text{B} \rightarrow \text{S}}^{[i]})$  and  $R_2 = \text{Rank}(\mathbf{H}_{\text{S} \rightarrow \text{UE}}^{[i,k]})$  denote the rank of matrices  $\mathbf{H}_{\text{B} \rightarrow \text{S}}^{[i]}$  and  $\mathbf{H}_{\text{S} \rightarrow \text{UE}}^{[i,k]}$ , respectively. Variables  $\gamma_{\text{B} \rightarrow \text{S},n}^{[i]}$  and  $\gamma_{\text{S} \rightarrow \text{UE},n}^{[i,k]}$  represent the equivalent channel-to-noise ratio (CNR) on spatial channel  $n$  in subcarrier  $i$  of the BS-to-SUDAS channel and the SUDAS-to-UE  $k$  channel, respectively. Similarly, we can exploit channel reciprocity and apply SVD to the UL two-hop channel matrices which yields

$$\begin{aligned} \mathbf{H}_{\text{S} \rightarrow \text{B}}^{[i]} &= \mathbf{V}_{\text{B} \rightarrow \text{S}}^{[i]} (\mathbf{\Lambda}_{\text{B} \rightarrow \text{S}}^{[i]})^H (\mathbf{U}_{\text{B} \rightarrow \text{S}}^{[i]})^H \quad \text{and} \\ \mathbf{H}_{\text{UE} \rightarrow \text{S}}^{[i,k]} &= \mathbf{V}_{\text{S} \rightarrow \text{UE}}^{[i,k]} (\mathbf{\Lambda}_{\text{S} \rightarrow \text{UE}}^{[i,k]})^H (\mathbf{U}_{\text{S} \rightarrow \text{UE}}^{[i,k]})^H. \end{aligned} \quad (29)$$

We are now ready to introduce the following theorem.

*Theorem 2:* Assuming that  $\text{Rank}(\mathbf{P}_{\text{DL}}^{[i,k]}) = \text{Rank}(\mathbf{P}_{\text{UL}}^{[i,k]}) = \text{Rank}(\mathbf{F}_{\text{DL}}^{[i,k]}) = \text{Rank}(\mathbf{F}_{\text{UL}}^{[i,k]}) = N_{\text{S}} \leq \min\{\text{Rank}(\mathbf{H}_{\text{S} \rightarrow \text{UE}}^{[i,k]}), \text{Rank}(\mathbf{H}_{\text{B} \rightarrow \text{S}}^{[i]})\}$ , the optimal linear precoding matrices used at the BS and the SUDACs for the maximization problem in (27) jointly diagonalize the DL and UL channels of the BS-SUDAS-UE link on each subcarrier, despite the non-convexity of the objective function<sup>7</sup>. The optimal precoding matrices have the following structure:

$$\mathbf{P}_{\text{DL}}^{[i,k]} = \tilde{\mathbf{V}}_{\text{B} \rightarrow \text{S}}^{[i]} \mathbf{\Lambda}_{\text{B,DL}}^{[i,k]}, \quad (30)$$

$$\mathbf{F}_{\text{DL}}^{[i,k]} = \tilde{\mathbf{V}}_{\text{S} \rightarrow \text{UE}}^{[i,k]} \mathbf{\Lambda}_{\text{F,DL}}^{[i,k]} (\tilde{\mathbf{U}}_{\text{B} \rightarrow \text{S}}^{[i,k]})^H, \quad (31)$$

$$\mathbf{P}_{\text{UL}}^{[i,k]} = \tilde{\mathbf{U}}_{\text{S} \rightarrow \text{UE}}^{[i]} \mathbf{\Lambda}_{\text{UE,UL}}^{[i,k]}, \quad \text{and} \quad (32)$$

$$\mathbf{F}_{\text{UL}}^{[i,k]} = \tilde{\mathbf{U}}_{\text{B} \rightarrow \text{S}}^{[i,k]} \mathbf{\Lambda}_{\text{F,UL}}^{[i,k]} (\tilde{\mathbf{V}}_{\text{S} \rightarrow \text{UE}}^{[i,k]})^H, \quad (33)$$

respectively, where  $\tilde{\mathbf{V}}_{\text{B} \rightarrow \text{S}}^{[i]}$ ,  $\mathbf{\Lambda}_{\text{UE,UL}}^{[i,k]}$ , and  $\tilde{\mathbf{U}}_{\text{B} \rightarrow \text{S}}^{[i,k]}$  are the  $N_{\text{S}}$  rightmost columns of  $\mathbf{V}_{\text{B} \rightarrow \text{S}}^{[i]}$ ,  $\mathbf{V}_{\text{S} \rightarrow \text{UE}}^{[i,k]}$ , and  $\mathbf{U}_{\text{B} \rightarrow \text{S}}^{[i]}$ , respectively. Matrices  $\mathbf{\Lambda}_{\text{B,DL}}^{[i,k]} \in \mathbb{C}^{N_{\text{S}} \times N_{\text{S}}}$ ,  $\mathbf{\Lambda}_{\text{F,DL}}^{[i,k]} \in \mathbb{C}^{N_{\text{S}} \times N_{\text{S}}}$ ,  $\mathbf{\Lambda}_{\text{B,UL}}^{[i,k]} \in \mathbb{C}^{N_{\text{S}} \times N_{\text{S}}}$ , and  $\mathbf{\Lambda}_{\text{F,UL}}^{[i,k]} \in \mathbb{C}^{N_{\text{S}} \times N_{\text{S}}}$  are diagonal matrices which

<sup>7</sup>We note that the diagonal structure is also optimal for frequency division duplex systems where  $\mathbf{H}_{\text{UE} \rightarrow \text{S}}^{[i,k]} \neq (\mathbf{H}_{\text{S} \rightarrow \text{UE}}^{[i,k]})^H$  and  $\mathbf{H}_{\text{S} \rightarrow \text{B}}^{[i]} \neq (\mathbf{H}_{\text{B} \rightarrow \text{S}}^{[i]})^H$ . Only the optimal precoding matrices in (30) and (32) will change accordingly to jointly diagonalize the end-to-end channel.

can be expressed as

$$\mathbf{\Lambda}_{\text{B}_{\text{DL}}}^{[i,k]} = \text{diag}(\mathbf{x}_{\text{B}_{\text{DL}}}^{[i,k]}), \quad \mathbf{\Lambda}_{\text{F}_{\text{DL}}}^{[i,k]} = \text{diag}(\mathbf{x}_{\text{F}_{\text{DL}}}^{[i,k]}), \quad (34)$$

$$\mathbf{\Lambda}_{\text{UE}_{\text{UL}}}^{[i,k]} = \text{diag}(\mathbf{x}_{\text{UE}_{\text{UL}}}^{[i,k]}), \quad \mathbf{\Lambda}_{\text{F}_{\text{UL}}}^{[i,k]} = \text{diag}(\mathbf{x}_{\text{F}_{\text{UL}}}^{[i,k]}), \quad (35)$$

$$\mathbf{x}_{\text{B}_{\text{DL}}}^{[i,k]} = \left[ \sqrt{P_{\text{B} \rightarrow \text{S},1}^{[i,k]}} \cdots \sqrt{P_{\text{B} \rightarrow \text{S},n}^{[i,k]}} \cdots \sqrt{P_{\text{B} \rightarrow \text{S},N_{\text{S}}}^{[i,k]}} \right], \quad (36)$$

$$\mathbf{x}_{\text{F}_{\text{DL}}}^{[i,k]} = \left[ \sqrt{P_{\text{S} \rightarrow \text{UE},1}^{[i,k]}} \cdots \sqrt{P_{\text{S} \rightarrow \text{UE},n}^{[i,k]}} \cdots \sqrt{P_{\text{S} \rightarrow \text{UE},N_{\text{S}}}^{[i,k]}} \right], \quad (37)$$

$$\mathbf{x}_{\text{UE}_{\text{UL}}}^{[i,k]} = \left[ \sqrt{P_{\text{UE} \rightarrow \text{S},1}^{[i,k]}} \cdots \sqrt{P_{\text{UE} \rightarrow \text{S},n}^{[i,k]}} \cdots \sqrt{P_{\text{UE} \rightarrow \text{S},N_{\text{S}}}^{[i,k]}} \right], \quad (38)$$

$$\text{and } \mathbf{x}_{\text{F}_{\text{UL}}}^{[i,k]} = \left[ \sqrt{P_{\text{S} \rightarrow \text{B},1}^{[i,k]}} \cdots \sqrt{P_{\text{S} \rightarrow \text{B},n}^{[i,k]}} \cdots \sqrt{P_{\text{S} \rightarrow \text{B},N_{\text{S}}}^{[i,k]}} \right], \quad (39)$$

respectively, where  $\text{diag}(x_1, \dots, x_K)$  denotes a diagonal matrix with diagonal elements  $\{x_1, \dots, x_K\}$ . Scalar optimization variables  $P_{\text{B} \rightarrow \text{S},n}^{[i,k]}$ ,  $P_{\text{S} \rightarrow \text{UE},n}^{[i,k]}$ ,  $P_{\text{UE} \rightarrow \text{S},n}^{[i,k]}$  and  $P_{\text{S} \rightarrow \text{B},n}^{[i,k]}$  are, respectively, the equivalent transmit powers of the BS-to-SUDAS link, the SUDAS-to-UE link, the UE-to-SUDAS link, and the SUDAS-to-BS link for UE  $k$  on spatial channel  $n$  and subcarrier  $i$ .

*Proof:* Please refer to the Appendix. ■

By adopting the optimal precoding matrices provided in Theorem 2, the DL and UL end-to-end channel on subcarrier  $i$  is converted into  $N_{\text{S}}$  parallel spatial channels. More importantly, the structure of the optimal precoding matrices simplifies the resource allocation algorithm design significantly as the matrix optimization variables can be replaced by equivalent scalar optimization variables. As a result, the achievable rates in DL and UL on subcarrier  $i$  from the BS to UE  $k$  via the SUDAS in (15) can be simplified as

$$R_{\text{DL}}^{[i,k]} = \sum_{n=1}^{N_{\text{S}}} \log_2 \left( 1 + \text{SINR}_{\text{DL}_n}^{[i,k]} \right),$$

$$\text{SINR}_{\text{DL}_n}^{[i,k]} = \frac{\gamma_{\text{B} \rightarrow \text{S},n}^{[i,k]} P_{\text{B} \rightarrow \text{S},n}^{[i,k]} P_{\text{S} \rightarrow \text{UE},n}^{[i,k]} \gamma_{\text{S} \rightarrow \text{UE},n}^{[i,k]}}{1 + \gamma_{\text{B} \rightarrow \text{S},n}^{[i,k]} P_{\text{B} \rightarrow \text{S},n}^{[i,k]} + P_{\text{S} \rightarrow \text{UE},n}^{[i,k]} \gamma_{\text{S} \rightarrow \text{UE},n}^{[i,k]}}, \quad (40)$$

$$R_{\text{UL}}^{[i,k]} = \sum_{n=1}^{N_{\text{S}}} \log_2 \left( 1 + \text{SINR}_{\text{UL}_n}^{[i,k]} \right),$$

$$\text{SINR}_{\text{UL}_n}^{[i,k]} = \frac{\gamma_{\text{S} \rightarrow \text{B},n}^{[i,k]} P_{\text{S} \rightarrow \text{B},n}^{[i,k]} P_{\text{UE} \rightarrow \text{S},n}^{[i,k]} \gamma_{\text{UE} \rightarrow \text{S},n}^{[i,k]}}{1 + \gamma_{\text{S} \rightarrow \text{B},n}^{[i,k]} P_{\text{S} \rightarrow \text{B},n}^{[i,k]} + P_{\text{UE} \rightarrow \text{S},n}^{[i,k]} \gamma_{\text{UE} \rightarrow \text{S},n}^{[i,k]}}, \quad (41)$$

where  $\text{SINR}_{\text{DL}_n}^{[i,k]}$  and  $\text{SINR}_{\text{UL}_n}^{[i,k]}$  are the received signal-to-interference-plus-noise-ratios (SINRs) at UE  $k$  and the BS in subcarrier  $i$  in spatial subchannel  $n \in \{1, \dots, N_{\text{S}}\}$ , respectively. Although the objective function is now a scalar function with respect to the optimization variables, it is still non-convex. To obtain a tractable resource allocation algorithm design, we propose the following objective function approximation. In particular, the end-to-end DL and UL SINRs on subcarrier

$i$  for UE  $k$  can be approximated, respectively, as

$$\begin{aligned} \text{SINR}_{\text{DL}_n}^{[i,k]} &\approx \overline{\text{SINR}}_{\text{DL}_n}^{[i,k]} \quad \text{and} \quad \text{SINR}_{\text{UL}_n}^{[i,k]} \approx \overline{\text{SINR}}_{\text{UL}_n}^{[i,k]}, \quad \text{where} \\ \overline{\text{SINR}}_{\text{DL}_n}^{[i,k]} &= \frac{\gamma_{\text{B} \rightarrow \text{S},n}^{[i,k]} P_{\text{B} \rightarrow \text{S},n}^{[i,k]} P_{\text{S} \rightarrow \text{UE},n}^{[i,k]} \gamma_{\text{S} \rightarrow \text{UE},n}^{[i,k]}}{\gamma_{\text{B} \rightarrow \text{S},n}^{[i,k]} P_{\text{B} \rightarrow \text{S},n}^{[i,k]} + P_{\text{S} \rightarrow \text{UE},n}^{[i,k]} \gamma_{\text{S} \rightarrow \text{UE},n}^{[i,k]}}, \\ \overline{\text{SINR}}_{\text{UL}_n}^{[i,k]} &= \frac{\gamma_{\text{S} \rightarrow \text{B},n}^{[i,k]} P_{\text{S} \rightarrow \text{B},n}^{[i,k]} P_{\text{UE} \rightarrow \text{S},n}^{[i,k]} \gamma_{\text{UE} \rightarrow \text{S},n}^{[i,k]}}{\gamma_{\text{S} \rightarrow \text{B},n}^{[i,k]} P_{\text{S} \rightarrow \text{B},n}^{[i,k]} + P_{\text{UE} \rightarrow \text{S},n}^{[i,k]} \gamma_{\text{UE} \rightarrow \text{S},n}^{[i,k]}}. \end{aligned} \quad (42)$$

We note that this approximation is asymptotically tight for high SNR<sup>8</sup> [26], [27].

The next step is to tackle the non-convexity due to combinatorial constraints C9 and C10 in (24). To this end, we adopt the time-sharing relaxation approach. In particular, we relax  $s_{\text{DL}}^{[i,k]}$  and  $s_{\text{UL}}^{[i,k]}$  in constraints C9 and C10 such that they are non-negative real valued optimization variables bounded from above by  $\alpha$  and  $\beta$ , respectively [30], i.e.,  $0 \leq s_{\text{DL}}^{[i,k]} \leq \alpha$  and  $0 \leq s_{\text{UL}}^{[i,k]} \leq \beta$ . It has been shown in [30] that the time-sharing relaxation is asymptotically optimal for a sufficiently large number of subcarriers<sup>9</sup>. Next, we define a set with four auxiliary optimization variables  $\tilde{\mathcal{P}} = \{\tilde{P}_{\text{B} \rightarrow \text{S},n}^{[i,k]}, \tilde{P}_{\text{UE} \rightarrow \text{S},n}^{[i,k]}, \tilde{P}_{\text{S} \rightarrow \text{UE},n}^{[i,k]}, \tilde{P}_{\text{S} \rightarrow \text{B},n}^{[i,k]}\}$  and rewrite the transformed objective function in (27) as:

$$\begin{aligned} \mathcal{U}_{\text{Trans}}(\tilde{\mathcal{P}}, \mathcal{S}) &= \sum_{k=1}^K \sum_{i=1}^{n_{\text{F}}} \sum_{n=1}^{N_{\text{S}}} \left\{ s_{\text{DL}}^{[i,k]} \log_2 \left( 1 + \frac{\widetilde{\text{SINR}}_{\text{DL}_n}^{[i,k]}}{s_{\text{DL}}^{[i,k]}} \right) \right. \\ &\quad \left. + s_{\text{UL}}^{[i,k]} \log_2 \left( 1 + \frac{\widetilde{\text{SINR}}_{\text{UL}_n}^{[i,k]}}{s_{\text{UL}}^{[i,k]}} \right) \right\} - \eta_{\text{eff}} \left( P_{\text{C}_{\text{B}}} + M P_{\text{C}_{\text{SUDAC}}} \right. \\ &\quad \left. + K P_{\text{C}_{\text{UE}}} + \sum_{k=1}^K \sum_{i=1}^{n_{\text{F}}} \sum_{n=1}^{N_{\text{S}}} \varepsilon_{\text{B}} \tilde{P}_{\text{B} \rightarrow \text{S},n}^{[i,k]} \right. \\ &\quad \left. + \varepsilon_{\text{S}} \tilde{P}_{\text{S} \rightarrow \text{UE},n}^{[i,k]} + \varepsilon_{\text{k}} \tilde{P}_{\text{UE} \rightarrow \text{S},n}^{[i,k]} + \varepsilon_{\text{S}} \tilde{P}_{\text{S} \rightarrow \text{B},n}^{[i,k]} \right) \end{aligned} \quad (43)$$

where  $\widetilde{\text{SINR}}_{\text{DL}_n}^{[i,k]} = \overline{\text{SINR}}_{\text{DL}_n}^{[i,k]} \Big|_{\tilde{\mathcal{P}}}$  and  $\tilde{\mathcal{P}} = \left\{ \tilde{P}_{\text{B} \rightarrow \text{S},n}^{[i,k]} = P_{\text{B} \rightarrow \text{S},n}^{[i,k]} s_{\text{DL}}^{[i,k]}, \tilde{P}_{\text{S} \rightarrow \text{UE},n}^{[i,k]} = P_{\text{S} \rightarrow \text{UE},n}^{[i,k]} s_{\text{DL}}^{[i,k]}, \tilde{P}_{\text{UE} \rightarrow \text{S},n}^{[i,k]} = P_{\text{UE} \rightarrow \text{S},n}^{[i,k]} s_{\text{UL}}^{[i,k]}, \tilde{P}_{\text{S} \rightarrow \text{B},n}^{[i,k]} = P_{\text{S} \rightarrow \text{B},n}^{[i,k]} s_{\text{UL}}^{[i,k]} \right\}$ . We note that the new auxiliary optimization variables in  $\tilde{\mathcal{P}}$  represent the actual transmit energy under the time-sharing condition. As a result, the combinatorial-constraint relaxed problem can be written

<sup>8</sup>It is expected that the high SNR assumption holds for the considered system due to the short distance communication between the SUDAS and the UEs, i.e.,  $P_{\text{S} \rightarrow \text{UE},n}^{[i,k]} \gamma_{\text{S} \rightarrow \text{UE},n}^{[i,k]}, P_{\text{UE} \rightarrow \text{S},n}^{[i,k]} \gamma_{\text{UE} \rightarrow \text{S},n}^{[i,k]} \gg 1$ .

<sup>9</sup>The duality gap due to the time-sharing relaxation is virtually zero for practical numbers of subcarriers, e.g.  $n_{\text{F}} \geq 8$  [31].

as:

$$\begin{aligned}
 & \text{maximize } \mathcal{U}_{\text{Trans}}(\tilde{\mathcal{P}}, \mathcal{S}) \\
 & \text{s.t. C1: } \sum_{k=1}^K \sum_{i=1}^{n_F} \sum_{n=1}^{N_S} \tilde{P}_{B \rightarrow S, n}^{[i, k]} \leq P_T, \\
 & \text{C2: } \sum_{k=1}^K \sum_{i=1}^{n_F} \sum_{n=1}^{N_S} \tilde{P}_{S \rightarrow \text{UE}, n}^{[i, k]} \leq MP_{\text{max}}, \\
 & \text{C3: } \sum_{i=1}^{n_F} \sum_{n=1}^{N_S} \tilde{P}_{\text{UE} \rightarrow S, n}^{[i, k]} \leq P_{\text{max}_k}, \forall k, \\
 & \text{C4: } \sum_{k=1}^K \sum_{i=1}^{n_F} \sum_{n=1}^{N_S} \tilde{P}_{S \rightarrow B, n}^{[i, k]} \leq P_{\text{max}}^{\text{UL}}, \\
 & \text{C5 - C8, C9: } 0 \leq s_{\text{DL}}^{[i, k]} \leq \alpha, \forall i, k, \\
 & \text{C10: } 0 \leq s_{\text{UL}}^{[i, k]} \leq \beta, \forall i, k, \text{ C11, C12.} \quad (44)
 \end{aligned}$$

Optimization problem (44) is jointly concave with respect to the auxiliary optimization variables  $\tilde{\mathcal{P}}$  and  $\mathcal{S}$ . We note that by solving optimization problem (44) for  $\tilde{P}_{B \rightarrow S}^{[i, k]}$ ,  $\tilde{P}_{S \rightarrow \text{UE}, n}^{[i, k]}$ ,  $\tilde{P}_{\text{UE} \rightarrow S, n}^{[i, k]}$ ,  $\tilde{P}_{S \rightarrow B, n}^{[i, k]}$ ,  $s_{\text{DL}}^{[i, k]}$ , and  $s_{\text{UL}}^{[i, k]}$ , we can recover the solution for  $P_{B \rightarrow S, n}^{[i, k]}$ ,  $P_{S \rightarrow \text{UE}, n}^{[i, k]}$ ,  $P_{\text{UE} \rightarrow S, n}^{[i, k]}$ , and  $P_{S \rightarrow B, n}^{[i, k]}$ . Thus, the solution of (44) is asymptotically optimal with respect to (24) for high SNR and sufficiently large numbers of subcarriers.

Now, we propose an algorithm for solving the transformed problem in (44). Although the transformed problem is jointly concave with respect to the optimization variables and can be solved by standard numerical methods such as interior point methods, this does not reveal the structure of the optimal solution and the interaction between different variables. Besides, the proposed asymptotically optimal resource allocation algorithm structure will serve as a building block for the design of a suboptimal resource allocation algorithm in the next section. The proposed iterative resource allocation algorithm is based on alternating optimization, standard optimization techniques, and the Karush-Kuhn-Tucker (KKT) conditions. The algorithm is summarized in Table II and is implemented by a repeated loop. In line 2, we first set the iteration index  $l$  to zero and initialize the resource allocation policy. Variables  $P_{B \rightarrow S, n}^{[i, k]}(l)$ ,  $P_{S \rightarrow \text{UE}, n}^{[i, k]}(l)$ ,  $P_{S \rightarrow B, n}^{[i, k]}(l)$ ,  $P_{\text{UE} \rightarrow S, n}^{[i, k]}(l)$ ,  $s_{\text{DL}}^{[i, k]}(l)$ ,  $s_{\text{UL}}^{[i, k]}(l)$ ,  $\alpha(l)$ , and  $\beta(l)$  denote the resource allocation policy in the  $l$ -th iteration. Then, in each iteration, we solve (44), which leads to (45)–(59):

$$P_{B \rightarrow S, n}^{[i, k]} = \left[ P_{S \rightarrow \text{UE}, n}^{[i, k]} \gamma_{S \rightarrow \text{UE}, n}^{[i, k]} \Upsilon_{B \rightarrow S, n}^{[i, k]} \right]^+, \quad (45)$$

$$\Upsilon_{B \rightarrow S, n}^{[i, k]} = \frac{\Omega_{B \rightarrow S, n}^{[i, k]} - \gamma_{S \rightarrow \text{UE}, n}^{[i, k]} P_{S \rightarrow \text{UE}, n}^{[i, k]} - 2}{2(\gamma_{B \rightarrow S, n}^{[i, k]} \gamma_{S \rightarrow \text{UE}, n}^{[i, k]} P_{S \rightarrow \text{UE}, n}^{[i, k]} + \gamma_{B \rightarrow S, n}^{[i, k]})}, \quad (46)$$

$$\Omega_{B \rightarrow S, n}^{[i, k]} = \frac{\sqrt{\Xi_{B \rightarrow S, n}^{[i, k]} + \Psi_{B \rightarrow S, n}^{[i, k]}}}{\sqrt{\lambda + \eta_{\text{eff}} \varepsilon_B \sqrt{\ln(2)}}}, \quad (47)$$

$$\Xi_{B \rightarrow S, n}^{[i, k]} = 4(1 + w_{\text{DL}}^{[i, k]}) \gamma_{B \rightarrow S, n}^{[i, k]} (1 + \gamma_{S \rightarrow \text{UE}, n}^{[i, k]} P_{S \rightarrow \text{UE}, n}^{[i, k]}), \quad (48)$$

$$\Psi_{B \rightarrow S, n}^{[i, k]} = (\gamma_{S \rightarrow \text{UE}, n}^{[i, k]})^2 (\lambda + \eta_{\text{eff}} \varepsilon_B) (P_{S \rightarrow \text{UE}, n}^{[i, k]})^2 \ln(2), \quad (49)$$

TABLE II  
ITERATIVE RESOURCE ALLOCATION ALGORITHM FOR SUDAS ASSISTED COMMUNICATION

**Algorithm 2** Alternating Optimization

- 1: Initialize the maximum number of iterations  $N_{\text{Iter}}^{\text{Alt}}$  and a small constant  $\kappa \rightarrow 0$
- 2: Set iteration index  $l = 0$  and initialize  $\{P_{B \rightarrow S, n}^{[i, k]}(l), P_{S \rightarrow \text{UE}, n}^{[i, k]}(l), s_{\text{DL}}^{[i, k]}(l)\}, \{P_{S \rightarrow B, n}^{[i, k]}(l), P_{\text{UE} \rightarrow S, n}^{[i, k]}(l), s_{\text{UL}}^{[i, k]}(l)\}, \alpha, \beta$ , and  $l = l + 1$
- 3: **repeat** {Loop}
- 4: For given  $P_{S \rightarrow \text{UE}, n}^{[i, k]}(l-1)$  and  $\alpha(l)$ , solve (44) for  $P_{B \rightarrow S, n}^{[i, k]}$  by using (45) which leads to intermediate power allocation variables  $P_{B \rightarrow S, n}^{[i, k]}'$
- 5: For given  $P_{B \rightarrow S, n}^{[i, k]}'$  and  $\alpha(l)$ , solve (44) for  $P_{S \rightarrow \text{UE}, n}^{[i, k]}$  via equation (50) which leads to intermediate power allocation variables  $P_{S \rightarrow \text{UE}, n}^{[i, k]}'$
- 6: Update the DL subcarrier allocation policy via (55) with  $P_{S \rightarrow \text{UE}, n}^{[i, k]}(l-1)$ ,  $P_{B \rightarrow S, n}^{[i, k]}'$ , and  $\alpha(l)$  to obtain the intermediate DL subcarrier allocation policy  $s_{\text{DL}}^{[i, k]}'(l)$
- 7: For given  $P_{S \rightarrow B, n}^{[i, k]}(l-1)$  and  $\beta(l)$ , solve (44) for  $P_{\text{UE} \rightarrow S, n}^{[i, k]}$  via equation (57) which leads to intermediate power allocation variables  $P_{\text{UE} \rightarrow S, n}^{[i, k]}'$
- 8: For given  $P_{\text{UE} \rightarrow S, n}^{[i, k]}'$  and  $\beta(l)$ , solve (44) for  $P_{S \rightarrow B, n}^{[i, k]}$  by using (59) which leads to intermediate power allocation variables  $P_{S \rightarrow B, n}^{[i, k]}'$
- 9: Update the UL subcarrier allocation policy via (67) with  $P_{S \rightarrow B, n}^{[i, k]}(l-1)$ ,  $P_{\text{UE} \rightarrow S, n}^{[i, k]}'$ , and  $\beta(l)$  to obtain the intermediate UL subcarrier allocation policy  $s_{\text{UL}}^{[i, k]}'(l)$
- 10: Update  $\alpha$  and  $\beta$  via standard linear programming methods to obtain intermediate solutions of  $\alpha'$  and  $\beta'$
- 11: **if**  $|P_{S \rightarrow \text{UE}, n}^{[i, k]}' - P_{S \rightarrow \text{UE}, n}^{[i, k]}(l-1)| \leq \kappa$ ,  $|P_{B \rightarrow S, n}^{[i, k]}' - P_{B \rightarrow S, n}^{[i, k]}(l-1)| \leq \kappa$ ,  $|s_{\text{DL}}^{[i, k]}' - s_{\text{DL}}^{[i, k]}(l-1)| \leq \kappa$ ,  $|P_{\text{UE} \rightarrow S, n}^{[i, k]}' - P_{\text{UE} \rightarrow S, n}^{[i, k]}(l-1)| \leq \kappa$ ,  $|P_{S \rightarrow B, n}^{[i, k]}' - P_{S \rightarrow B, n}^{[i, k]}(l-1)| \leq \kappa$ ,  $|s_{\text{UL}}^{[i, k]}' - s_{\text{UL}}^{[i, k]}(l-1)| \leq \kappa$ ,  $|\alpha' - \alpha(l-1)| \leq \kappa$ , and  $|\beta' - \beta(l-1)| \leq \kappa$  **then**
- 12:     Convergence = **true**, **return**  $\{P_{S \rightarrow \text{UE}, n}^{[i, k]}'$ ,  $P_{B \rightarrow S, n}^{[i, k]}'$ ,  $s_{\text{DL}}^{[i, k]}'$ ,  $P_{\text{UE} \rightarrow S, n}^{[i, k]}'$ ,  $P_{S \rightarrow B, n}^{[i, k]}'$ ,  $s_{\text{UL}}^{[i, k]}'$ ,  $\alpha'$ ,  $\beta'\}$
- 13: **else**
- 14:     Convergence = **false**,  $P_{S \rightarrow \text{UE}, n}^{[i, k]}(l) = P_{S \rightarrow \text{UE}, n}^{[i, k]}'$ ,  $P_{B \rightarrow S, n}^{[i, k]}(l) = P_{B \rightarrow S, n}^{[i, k]}'$ ,  $s_{\text{DL}}^{[i, k]}(l) = s_{\text{DL}}^{[i, k]}'$ ,  $P_{\text{UE} \rightarrow S, n}^{[i, k]}(l) = P_{\text{UE} \rightarrow S, n}^{[i, k]}'$ ,  $P_{S \rightarrow B, n}^{[i, k]}(l) = P_{S \rightarrow B, n}^{[i, k]}'$ ,  $s_{\text{UL}}^{[i, k]}(l) = s_{\text{UL}}^{[i, k]}'$ ,  $\alpha(l) = \alpha'$ ,  $\beta(l) = \beta'$ ,  $l = l + 1$
- 15:     **end if**
- 16: **until**  $l = N_{\text{Iter}}^{\text{Alt}}$

with  $P_{S \rightarrow \text{UE}, n}^{[i, k]}(l-1)$  and  $\alpha(l)$  from the last iteration, where  $[x]^+ = \max\{x, 0\}$ . Then, the obtained intermediate power allocation variable  $P_{B \rightarrow S, n}^{[i, k]}$  is used as an input for solving

(44) for  $P_{S \rightarrow UE,n}^{[i,k]}$  via the following equations:

$$P_{S \rightarrow UE,n}^{[i,k]} = \left[ \gamma_{B \rightarrow S,n}^{[i]} P_{B \rightarrow S,n}^{[i,k]} \Upsilon_{S \rightarrow UE,n}^{[i,k]} \right]^+, \quad (50)$$

$$\Upsilon_{S \rightarrow UE,n}^{[i,k]} = \frac{\left( \Omega_{S \rightarrow UE,n}^{[i,k]} - \gamma_{B \rightarrow S,n}^{[i]} P_{B \rightarrow S,n}^{[i,k]} - 2 \right)}{2(\gamma_{B \rightarrow S,n}^{[i]} \gamma_{S \rightarrow UE,n}^{[i,k]} P_{B \rightarrow S,n}^{[i,k]} + \gamma_{S \rightarrow UE,n}^{[i,k]})}, \quad (51)$$

$$\Omega_{S \rightarrow UE,n}^{[i,k]} = \frac{\sqrt{\Xi_{S \rightarrow UE,n}^{[i,k]} + \Psi_{S \rightarrow UE,n}^{[i,k]}}}{\sqrt{\delta + \eta_{\text{eff}} \varepsilon_S \sqrt{\ln(2)}}}, \quad (52)$$

$$\Xi_{S \rightarrow UE,n}^{[i,k]} = (\gamma_{B \rightarrow S,n}^{[i]})^2 (\delta + \eta_{\text{eff}} \varepsilon_S) (P_{B \rightarrow S,n}^{[i,k]})^2 \ln(2), \quad (53)$$

$$\Psi_{S \rightarrow UE,n}^{[i,k]} = (\gamma_{B \rightarrow S,n}^{[i]} P_{B \rightarrow S,n}^{[i,k]} + 1) 4(1 + w_{\text{DL}}^{[k]}) \gamma_{S \rightarrow UE,n}^{[i,k]}. \quad (54)$$

Eqs. (45)–(54) are obtained by standard convex optimization techniques.  $\lambda$  and  $\delta$  in (47) and (52) are the Lagrange multipliers for constraints C1 and C2 in (44), respectively. In particular,  $\lambda$  and  $\delta$  are monotonically decreasing with respect to  $P_{B \rightarrow S,n}^{[i,k]}$  and  $P_{S \rightarrow UE,n}^{[i,k]}$ , respectively, and control the transmit power at the BS and the SUDAS to satisfy constraints C1 and C2, respectively. Besides,  $w_{\text{DL}}^{[k]} \geq 0$  is the Lagrange multiplier associated with the minimum required DL data rate constraint C5 for delay sensitive UE  $k$ . The optimal values of  $\lambda$ ,  $\delta$ , and  $w_{\text{DL}}^{[k]}$  in each iteration can be found by a standard gradient algorithm such that constraints C1, C2, and C4 in (44) are satisfied. Variable  $\eta_{\text{eff}} \geq 0$  generated by the Dinkelbach method prevents unnecessary energy expenditures by reducing the values of  $\Omega_{B \rightarrow S,n}^{[i,k]}$  and  $\Omega_{S \rightarrow UE,n}^{[i,k]}$  in (47) and (52), respectively. Besides, the power allocation strategy in (45) and (50) is analogous to the water-filling solution in traditional single-hop communication systems. In particular,  $\Omega_{S \rightarrow UE,n}^{[i,k]}$  and  $\Omega_{B \rightarrow S,n}^{[i,k]}$  act as water levels for controlling the allocated power. Interestingly, the water level in the power allocation for the BS-to-SUDAS link depends on the associated channel gain which is different from the power allocation in non-SUDAS assisted communication [14], [15]. Furthermore, it can be seen from (47) and (52) that the water levels of different users can be different. Specifically, if the end-to-end channel gains of two users are the same, to satisfy the data rate requirement, the water level of a delay-sensitive user is generally higher than that of a non-delay sensitive user.

After obtaining the intermediate DL power allocation policy, cf. lines 4, 5, we update the DL subcarrier allocation, cf. line 6, as:

$$s_{\text{DL}}^{[i,k]} = \begin{cases} \alpha & \text{if } k = \arg \max_{t \in \{1, \dots, K\}} M_{\text{DL}}^{[i,t]} \\ 0 & \text{otherwise} \end{cases}, \quad (55)$$

where

$$M_{\text{DL}}^{[i,k]} = (1 + w_{\text{DL}}^{[t]}) \left( \sum_{n=1}^N \log_2 \left( 1 + \overline{\text{SINR}}_{\text{DL}_n}^{[i,t]} \right) - \frac{\overline{\text{SINR}}_{\text{DL}_n}^{[i,t]}}{1 + \overline{\text{SINR}}_{\text{DL}_n}^{[i,t]}} \right). \quad (56)$$

Here,  $\overline{\text{SINR}}_{\text{DL}_n}^{[i,k]}$  is obtained by substituting the intermediate solution of  $P_{B \rightarrow S,n}^{[i,k]}$  and  $P_{S \rightarrow UE,n}^{[i,k]}$ , i.e., (45) and (50), into (42) in the  $l$ -th iteration. We note that the optimal value of  $s_{\text{DL}}^{[i,k]}$

of the relaxed problem is a discrete value, cf. (55), i.e., the constraint relaxation is tight.

Similarly, we optimize the UL power allocation variables,  $P_{UE \rightarrow S,n}^{[i,k]}$  and  $P_{S \rightarrow B,n}^{[i,k]}$ , sequentially, cf. lines 7, 8, via the following equations:

$$P_{UE \rightarrow S,n}^{[i,k]} = \left[ \gamma_{S \rightarrow B,n}^{[i]} P_{S \rightarrow B,n}^{[i,k]} \Upsilon_{UE \rightarrow S,n}^{[i,k]} \right]^+, \quad (57)$$

$$\Upsilon_{UE \rightarrow S,n}^{[i,k]} = \frac{\left( \Omega_{UE \rightarrow S,n}^{[i,k]} - \gamma_{S \rightarrow B,n}^{[i]} P_{S \rightarrow B,n}^{[i,k]} - 2 \right)}{2(\gamma_{S \rightarrow B,n}^{[i]} \gamma_{UE \rightarrow S,n}^{[i,k]} P_{S \rightarrow B,n}^{[i,k]} + \gamma_{UE \rightarrow S,n}^{[i,k]})}, \quad (58)$$

$$P_{S \rightarrow B,n}^{[i,k]} = \left[ \gamma_{UE \rightarrow S,n}^{[i,k]} P_{UE \rightarrow S,n}^{[i,k]} \Upsilon_{S \rightarrow B,n}^{[i,k]} \right]^+, \quad (59)$$

$$\Upsilon_{S \rightarrow B,n}^{[i,k]} = \frac{\left( \Omega_{S \rightarrow B,n}^{[i,k]} - \gamma_{UE \rightarrow S,n}^{[i,k]} P_{UE \rightarrow S,n}^{[i,k]} - 2 \right)}{2(\gamma_{S \rightarrow B,n}^{[i]} \gamma_{UE \rightarrow S,n}^{[i,k]} P_{UE \rightarrow S,n}^{[i,k]} + \gamma_{S \rightarrow B,n}^{[i]})}, \quad (60)$$

respectively, where

$$\Omega_{UE \rightarrow S,n}^{[i,k]} = \frac{\sqrt{\Xi_{UE \rightarrow S,n}^{[i,k]} + \Psi_{UE \rightarrow S,n}^{[i,k]}}}{\sqrt{\psi_k + \eta_{\text{eff}} \varepsilon_k \sqrt{\ln(2)}}}, \quad (61)$$

$$\Xi_{UE \rightarrow S,n}^{[i,k]} = (\gamma_{S \rightarrow B,n}^{[i]})^2 (\psi_k + \eta_{\text{eff}} \varepsilon_k) (P_{S \rightarrow B,n}^{[i,k]})^2 \ln(2), \quad (62)$$

$$\Psi_{UE \rightarrow S,n}^{[i,k]} = (\gamma_{S \rightarrow B,n}^{[i]} P_{S \rightarrow B,n}^{[i,k]} + 1) 4(1 + w_{\text{UL}}^{[k]}) \gamma_{UE \rightarrow S,n}^{[i,k]}, \quad (63)$$

$$\Omega_{S \rightarrow B,n}^{[i,k]} = \frac{\sqrt{\Xi_{S \rightarrow B,n}^{[i,k]} + \Psi_{S \rightarrow B,n}^{[i,k]}}}{\sqrt{\phi + \eta_{\text{eff}} \varepsilon_S \sqrt{\ln(2)}}}, \quad (64)$$

$$\Xi_{S \rightarrow B,n}^{[i,k]} = 4(1 + w_{\text{UL}}^{[k]}) \gamma_{S \rightarrow B,n}^{[i]} (1 + \gamma_{UE \rightarrow S,n}^{[i,k]} P_{UE \rightarrow S,n}^{[i,k]}), \quad (65)$$

$$\Psi_{S \rightarrow B,n}^{[i,k]} = (\gamma_{UE \rightarrow S,n}^{[i,k]})^2 (\phi + \eta_{\text{eff}} \varepsilon_S) (P_{UE \rightarrow S,n}^{[i,k]})^2 \ln(2). \quad (66)$$

$\psi_k$  and  $\phi$  in (61) and (64) are the Lagrange multipliers with respect to power consumption constraints C3 and C4 in (44), respectively. Besides,  $w_{\text{UL}}^{[k]}$  is the Lagrange multiplier associated with the minimum required UL data rate constraint C6 for delay sensitive UE  $k$ . The optimal values of  $\psi_k$ ,  $\phi$ , and  $w_{\text{UL}}^{[k]}$  in each iteration can be easily obtained again with a standard gradient algorithm such that constraints C3, C4, and C6 in (44) are satisfied.

Then, we update the UL subcarrier allocation policy  $s_{\text{UL}}^{[i,k]}$  via

$$s_{\text{UL}}^{[i,k]} = \begin{cases} \beta & \text{if } k = \arg \max_{t \in \{1, \dots, K\}} M_{\text{UL}}^{[i,t]} \\ 0 & \text{otherwise} \end{cases}, \quad (67)$$

$$M_{\text{UL}}^{[i,k]} = (1 + w_{\text{UL}}^{[t]}) \left( \sum_{n=1}^N \log_2 \left( 1 + \overline{\text{SINR}}_{\text{UL}_n}^{[i,t]} \right) - \frac{\overline{\text{SINR}}_{\text{UL}_n}^{[i,t]}}{1 + \overline{\text{SINR}}_{\text{UL}_n}^{[i,t]}} \right),$$

where  $\overline{\text{SINR}}_{\text{UL}_n}^{[i,k]}$  is obtained by substituting the intermediate solutions for  $P_{UE \rightarrow S,n}^{[i,k]}$  and  $P_{S \rightarrow B,n}^{[i,k]}$ , i.e., (57) and (59), into (42) in the  $l$ -th iteration. Again, the constraint relaxation is tight.

Subsequently, for a given UL and DL power allocation policy and given  $s_{\text{DL}}^{[i,k]}$  and  $s_{\text{UL}}^{[i,k]}$ , the optimization problem is a linear programming with respect to  $\alpha$  and  $\beta$ . Thus, we can update  $\alpha$  and  $\beta$  via standard linear programming methods to obtain intermediate solutions for  $\alpha'$  and  $\beta'$  [32]. Then, the

overall procedure is repeated iteratively until we reach the maximum number of iterations or convergence is achieved. We note that for a sufficient number of iterations, the convergence to the optimal solution of (44) is guaranteed since (44) is jointly concave with respect to the optimization variables [33].

### C. Suboptimal Solution

In the last section, we proposed an asymptotically globally optimal algorithm based on the high SNR assumption. In this section, we propose a suboptimal resource allocation algorithm which achieves a local optimal solution of (24) for arbitrary SNR values. Similar to the asymptotically optimal solution, we apply Theorem 1, Theorem 2, and Algorithm 1 to simplify the power allocation and subcarrier allocation. In particular, the DL and UL data rates of UE  $k$  on subcarrier  $i$  are given by (40) and (41), respectively. It can be observed that (40) and (41) are concave functions with respect to  $P_{B \rightarrow S,n}^{[i,k]}$ ,  $P_{S \rightarrow B,n}^{[i,k]}$ ,  $P_{S \rightarrow UE,n}^{[i,k]}$ , and  $P_{UE \rightarrow S,n}^{[i,k]}$  individually, when the other variables are fixed. Thus, we can apply alternating optimization to obtain a local optimal solution [33] of (24). We note that unlike the proposed asymptotically optimal scheme, the high SNR assumption is not required to convexify the problem. The suboptimal solution can be obtained by Algorithm 2 in Table II, but now, we update the power allocation variables, i.e., lines 4, 5, 7, 8, in Algorithm 2, by using equations (68)–(71) on the top of next page, which are obtained by applying standard optimization techniques [27]. Besides, the subcarrier allocation policies for DL and UL are still given by (55) and (67), respectively, except that we replace  $\overline{\text{SINR}}_{DL,n}^{[i,k]}$ ,  $\overline{\text{SINR}}_{UL,n}^{[i,k]}$  by  $\text{SINR}_{DL,n}^{[i,k]}$ ,  $\text{SINR}_{UL,n}^{[i,k]}$  in (42). The optimization variables are updated repeatedly until convergence or the maximum number of iterations is reached. In contrast to the asymptotically optimal algorithm in Section IV-B, which may not even achieve a locally optimal solution for finite SNRs, the suboptimal iterative algorithm is guaranteed to converge to a local optimum [33] for arbitrary SNR values.

*Remark 4:* The problem formulation in (24) focuses on energy efficiency maximization but is in fact very general. For example, by setting  $\alpha = 0$ ,  $\beta = 1$ , and  $R_{\min,k}^{\text{DL}} = 0$  in (24), the proposed optimization problem becomes an uplink energy efficiency maximization problem for the proposed SUDAS. Besides, the proposed problem formulation is also a generalization of network throughput maximization and total power minimization, respectively. Indeed, the value of  $\eta_{\text{eff}}$  in (27) can be interpreted as the penalty to the energy efficiency due to exceedingly high power consumption. If we force  $\eta_{\text{eff}}^* = 0$ , i.e., there is no penalty in using exceedingly high power, then the transformed optimization problem  $\max_{\{\mathcal{P}, \mathcal{S}\} \in \mathcal{F}} \mathcal{U}(\mathcal{P}, \mathcal{S}) - \eta_{\text{eff}}^* \mathcal{U}_{\text{TP}}(\mathcal{P}, \mathcal{S})$  becomes a network aggregate throughput maximization problem. Besides, it is known that throughput maximization and power minimization are dual to each other [34]. In other words, the solution structure of our energy-efficiency maximization problem can also be used to solve the throughput maximization and power minimization problems by making some appropriate modifications [34].

### D. Computational Complexity

In this section, we study the computational complexity of the proposed asymptotically optimal and suboptimal algorithms. The computational complexity analysis of the proposed optimal algorithm can be divided into two parts. The first part concerns the computational complexity of the singular value decomposition (SVD) which can be upper bounded as [35, Chapter 4.1]

$$\mathcal{O}(MN^2 + N^3). \quad (72)$$

For the second part, we assume that quick sort is employed for the subcarrier allocation in equations (55) and (67) and the subgradient method is adopted to find the optimal Lagrange multipliers. Combining these two parts, a computational complexity upper bound for the proposed asymptotically optimal solution is given by:

$$\begin{aligned} & \underbrace{\mathcal{O}((K+1) \times n_F \times (MN^2 + N^3))}_{\text{SVD}} \\ & + N_{\text{Iter}}^{\text{Dinkelbach}} \left\{ N_{\text{Iter}}^{\text{Alt}} \left\{ N_{\text{Iter}}^{\text{Grad}} \left( \underbrace{\mathcal{O}(2 \times n_F \times K \log K)}_{\text{subcarrier allocation}} \right. \right. \right. \\ & \left. \left. \left. + \underbrace{\mathcal{O}(2 \times n_F \times (K+1) \times n_S)}_{\text{power allocation}} + \underbrace{\mathcal{O}\left(\frac{3K+5}{\delta^2}\right)}_{\text{subgradient}} \right) \right\} \right\} \quad (73) \end{aligned}$$

where  $\mathcal{O}(\cdot)$  is the big-O notation. Constants  $N_{\text{Iter}}^{\text{Dinkelbach}}$ ,  $N_{\text{Iter}}^{\text{Alt}}$ ,  $N_{\text{Iter}}^{\text{Grad}}$ , and  $\delta > 0$  denote the number of iterations for the Dinkelbach method, the number of iterations for alternating optimization, the number of iterations for subgradient method, and the solution accuracy, respectively. In (73), the factor  $3K + 5$  is the number of dual variables to be updated by the subgradient method. On the other hand, the proposed suboptimal algorithm has the same computational complexity as the asymptotically optimal algorithm. We note that both of the proposed algorithms are polynomial time computational complexity algorithms which are considered to be fast algorithms in the literature [36, Chapter 34] and are desirable for real-time implementation.

## V. RESULTS AND DISCUSSION

In this section, we evaluate the system performance based on Monte Carlo simulations. We assume an indoor environment with  $K = 4$  UEs and  $M$  SUDACs and an outdoor BS. The distances between the BS and UEs and between each SUDAS and each UE are 100 meters and 4 meters, respectively. For the BS-to-SUDAS links, we adopt the Urban macro outdoor-to-indoor scenario of the Wireless World Initiative New Radio (WINNER+) channel model [37]. The center frequency and the bandwidth of the licensed band are 800 MHz and 20 MHz, respectively. There are  $n_F = 1200$  subcarriers with 15 kHz subcarrier bandwidth resulting in 18 MHz signal bandwidth for data transmission<sup>10</sup>. Hence, the BS-to-SUDAS link configuration is in accordance with

<sup>10</sup>The proposed SUDAS can be easily extended to the case when carrier aggregation is implemented at the BS to create a large signal bandwidth ( $\sim 100$  MHz) in the licensed band.

$$P_{B \rightarrow S,n}^{[i,k]} = \frac{1}{\gamma_{B \rightarrow S,n}^{[i]}} \left[ \frac{P_{S \rightarrow UE,n}^{[i,k]} \gamma_{S \rightarrow UE,n}^{[i,k]}}{2} \left( \sqrt{1 + \frac{4\gamma_{B \rightarrow S,n}^{[i]}(1 + w_{DL}^{[k]})}{\gamma_{S \rightarrow UE,n}^{[i]} P_{S \rightarrow UE,n}^{[i,k]} \ln(2)(\lambda + \eta_{eff} \epsilon_B)}} - 1 \right) - 1 \right]^+, \quad (68)$$

$$P_{S \rightarrow UE,n}^{[i,k]} = \frac{1}{\gamma_{S \rightarrow UE,n}^{[i,k]}} \left[ \frac{P_{B \rightarrow S,n}^{[i,k]} \gamma_{B \rightarrow S,n}^{[i]}}{2} \left( \sqrt{1 + \frac{4\gamma_{S \rightarrow UE,n}^{[i,k]}(1 + w_{DL}^{[k]})}{\gamma_{B \rightarrow S,n}^{[i]} P_{B \rightarrow S,n}^{[i,k]} \ln(2)(\delta + \eta_{eff} \epsilon_S)}} - 1 \right) - 1 \right]^+, \quad (69)$$

$$P_{S \rightarrow B,n}^{[i,k]} = \frac{1}{\gamma_{S \rightarrow B,n}^{[i]}} \left[ \frac{P_{UE \rightarrow S,n}^{[i,k]} \gamma_{UE \rightarrow S,n}^{[i,k]}}{2} \left( \sqrt{1 + \frac{4\gamma_{S \rightarrow B,n}^{[i]}(1 + w_{UL}^{[k]})}{\gamma_{UE \rightarrow S,n}^{[i]} P_{UE \rightarrow S,n}^{[i,k]} \ln(2)(\phi + \eta_{eff} \epsilon_S)}} - 1 \right) - 1 \right]^+, \quad (70)$$

$$P_{UE \rightarrow S,n}^{[i,k]} = \frac{1}{\gamma_{UE \rightarrow S,n}^{[i,k]}} \left[ \frac{P_{S \rightarrow B,n}^{[i,k]} \gamma_{S \rightarrow B,n}^{[i]}}{2} \left( \sqrt{1 + \frac{4\gamma_{UE \rightarrow S,n}^{[i,k]}(1 + w_{UL}^{[k]})}{\gamma_{S \rightarrow B,n}^{[i]} P_{S \rightarrow B,n}^{[i,k]} \ln(2)(\psi_k + \eta_{eff} \epsilon_k)}} - 1 \right) - 1 \right]^+. \quad (71)$$

the system parameters adopted in the Long Term Evolution (LTE) standard [38]. As for the SUDAS-to-UE links, we adopt the IEEE 802.11ad channel model [39] in the range of 60 GHz and assume that  $M$  orthogonal sub-bands are available. The maximum transmit power of the SUDACs and UEs is set to  $MP_{\max} = P_{\max}^{UL} = P_{\max_k} = 23$  dBm which is in accordance with the maximum power spectral density suggested by the Harmonized European Standard for the mmW frequency band, i.e., 13 dBm-per-MHz, and the typical maximum transmit power budgets of the UEs. For simplicity, we assume that  $N_S = \min\{N, M\}$  for studying the system performance. We model the SUDAS-to-BS and UE-to-SUDAS links as the conjugate transpose of the BS-to-SUDAS and SUDAS-to-UE links, respectively. Also, the power amplifier efficiencies of all power amplifiers are set to 25%. The circuit power consumption for the BS and each BS antenna are given by  $P_{CB} = 15$  Watt and  $P_{AntB} = 0.975$  Watt, respectively [40], [41]. The circuit power consumptions per SUDAC and UE are set to  $P_{CSUDAC} = 0.1$  Watt [42] and  $P_{CUE} = 1$  Watt, respectively. We assume that there is always one delay sensitive UE requiring  $R_{\min_k}^{DL} = 20$  Mbit/s and  $R_{\min_k}^{UL} = 20$  Mbit/s in DL and UL, respectively. Also,  $N_S$  is chosen as  $N_S = \min\{\text{Rank}(\mathbf{H}_{S \rightarrow UE}^{[i,k]}), \text{Rank}(\mathbf{H}_{B \rightarrow S}^{[i]})\}$ . All results were averaged over 10000 different multipath fading channel realizations.

#### A. Convergence of the Proposed Iterative Algorithm

Figure 3 illustrates the convergence of the proposed optimal and suboptimal algorithms for  $N = 8$  antennas at the BS,  $M = 8$  SUDACs, and different maximum transmit powers at the BS,  $P_T$ . We compare the system performance of the proposed algorithms with a performance upper bound which is obtained by computing the optimal objective value in (44) for noise-free reception at the UEs and the BS. The performance gap between the asymptotically optimal performance and the upper bound constitutes an upper bound on the performance loss due to the high SINR approximation adopted in (42). The number of iterations is defined as the aggregate number of iterations required by Algorithms 1 and 2. It can be observed that the proposed asymptotically optimal algorithm approaches 99% of the upper bound value after 20 iterations which confirms

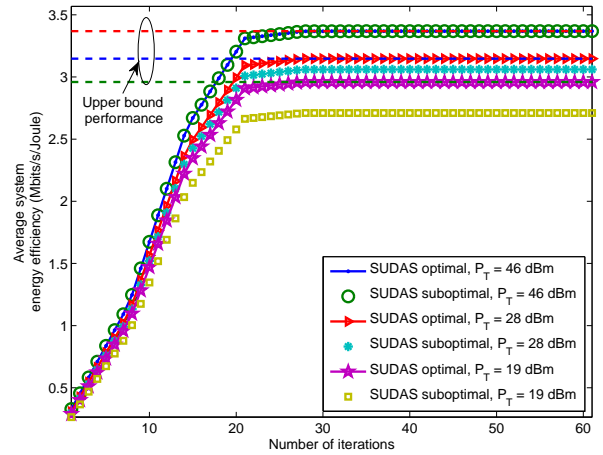


Fig. 3. Average energy efficiency (Mbits/Joule) versus the number of iterations for different maximum transmit power budgets at the BS.

the practicality of the proposed iterative algorithm. Besides, the suboptimal resource allocation algorithm achieves 90% of the upper bound value in the low transmit power regime, i.e.,  $P_T = 19$  dBm, and virtually the same energy efficiency as the upper bound performance in the high transmit power regime, i.e.,  $P_T = 46$  dBm. In the following case studies, the number of iterations is set to 30 in order to illustrate the performance of the proposed algorithms.

#### B. Average System Energy Efficiency versus Maximum Transmit Power

Figure 4 illustrates the average system energy efficiency versus the maximum DL transmit power at the BS for  $M = 8$  SUDACs for different systems and  $N = 8$  BS antennas. It can be observed that the average system energy efficiency of the two proposed resource allocation algorithms for SUDAS is a monotonically non-decreasing function of  $P_T$ . In particular, starting from a small value of  $P_T$ , the energy efficiency increases slowly with increasing  $P_T$  and then saturates when  $P_T > 37$  dBm. This is due to the fact that the two proposed algorithms strike a balance between system energy efficiency and power consumption. In fact, once the maximum energy

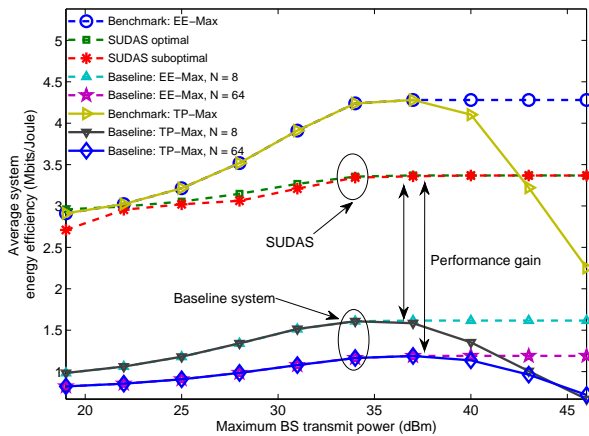


Fig. 4. Average energy efficiency (Mbits/Joule) versus the maximum transmit power at the BS (dBm) for different communication systems. The double-sided arrows indicate the performance gain achieved by the proposed SUDAS.

efficiency of the SUDAS is achieved, even if there is more power available for transmission, the BS will not consume extra DL transmit power for improving the data rate, cf. (45). This is because a further increase in the BS transmit power would only result in a degradation of the energy efficiency. Moreover, we compare the energy efficiency of the proposed SUDAS with a benchmark MIMO system and a baseline system. We focus on two system design objectives for the reference systems, namely, system throughput maximization (TP-Max) and energy efficiency maximization (EE-Max). For the benchmark MIMO system, we assume that each UE is equipped with  $N$  receive antennas but the SUDAS is not used and optimal resource allocation is performed<sup>11</sup>. The benchmark system also utilizes simultaneously the licensed and the unlicensed frequency bands via two carriers. Besides, we assume that the corresponding circuit power consumption at the UE does not scale with the number of antennas. In other words, the average system energy efficiency of the benchmark system serves as a performance upper bound for the proposed SUDAS. For the baseline system, we assume that the BS and the single-antenna UEs perform optimal resource allocation and utilize the licensed and the unlicensed frequency band<sup>12</sup>, i.e., the SUDAS is not used. As can be observed from Figure 4, for high BS transmit power budgets, the SUDAS achieves more than 80% of the performance of the benchmark MIMO system even though the UEs are only equipped with single antennas. Also, the SUDAS provides a huge system performance gain compared to the baseline system which does not employ SUDAS since the proposed SUDAS allows the single-antenna UEs to exploit spatial and frequency multiplexing gains. On the other hand, increasing

<sup>11</sup>The optimal resource allocation for the benchmark system can be obtained by following a similar method as the one proposed in this paper applying also fractional programming and majorization theory.

<sup>12</sup>We note that since the signal in the unlicensed frequency band, i.e., 60 GHz band, is highly attenuated by walls/obstructals, the use of unlicensed bands without SUDAS for outdoor-to-indoor communications can offer only negligible gain.

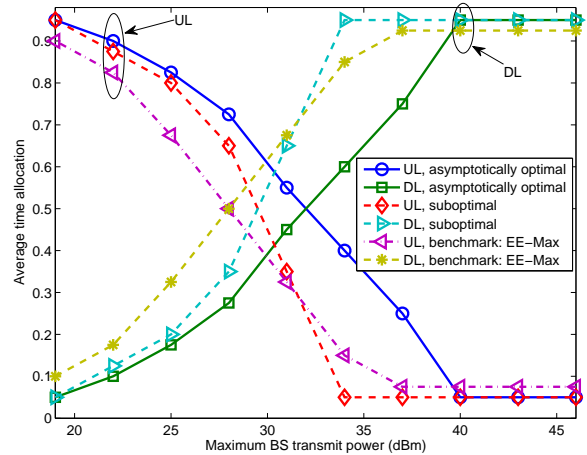


Fig. 5. Average DL and UL transmission durations versus the maximum transmit power at the BS (dBm).

the number of BS antennas dramatically in the baseline system from  $N = 8$  to  $N = 64$ , i.e., to a large-scale antenna system, does not necessarily improve the system energy efficiency. In fact, in the baseline system, the higher power consumption, which increases linearly with the number of BS antennas, outweighs the system throughput gain, which scales only logarithmically with the additional BS antennas.

Figure 5 depicts the average time allocation for DL and UL transmission. It can be observed that the optimal time allocation depends on the transmit power budget of the systems. In particular, when the power budget of the BS for DL communication is small compared to the total transmit power budget for UL communication, e.g.  $P_T \leq 28$  dBm, the period of time allocated for DL transmission is shorter than that allocated for UL transmission. Because of the limited power budget and the circuit power consumption, it is preferable for the BS to transmit a sufficiently large power over a short period of time rather than a small power over a longer time to maximize the system energy efficiency and to fulfill the data rate requirement of the DL delay sensitive UEs. On the contrary, when the power budget of the BS is large compared to that of the UEs, the system allocates more time resources to the DL compared to the UL, since the BS can now transmit a large enough power to compensate the circuit power consumption for a longer time span to maximize the system energy efficiency.

### C. Average System Throughput versus Maximum Transmit Power

Figure 6 illustrates the average system throughput versus the maximum transmit power at the BS for  $N = 8$  BS antennas,  $K = 4$  UEs, and  $M = 8$ . We compare the two proposed algorithms with the two aforementioned reference systems. The proposed SUDAS performs close to the benchmark scheme in the low DL transmit power budget regime, e.g.  $P_T \leq 31$  dBm. This is due to the fact that the proposed SUDAS allows the single-antenna UEs to transmit or receive multiple parallel

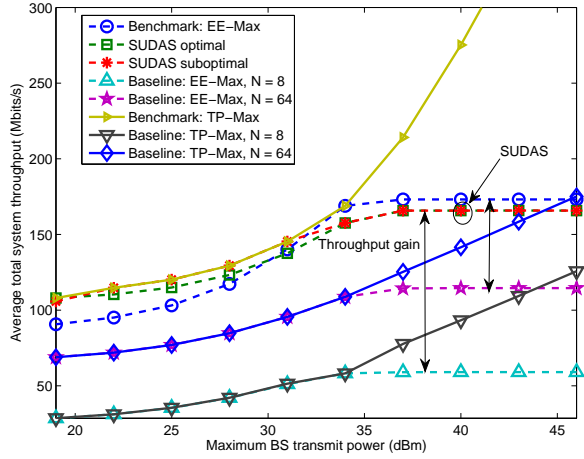


Fig. 6. Average system throughput (Mbits/s) versus the maximum transmit power at the BS (dBm).

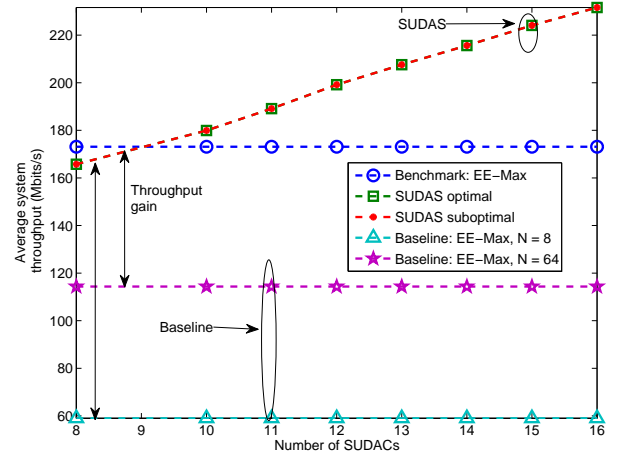


Fig. 8. Average system throughput (Mbits/s) versus the number of SUDACs.

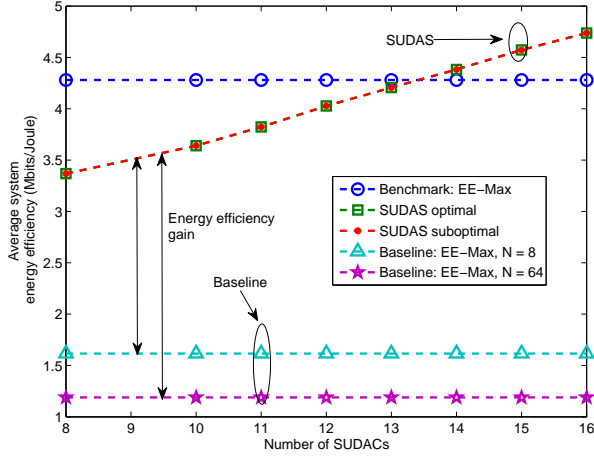


Fig. 7. Average energy efficiency (Mbits/Joule) versus the number of SUDACs.

data streams by utilizing the large bandwidth available in the unlicensed band. Besides, for all considered systems, the average system throughput increases monotonically with the maximum DL transmit power  $P_T$ . Yet, for the systems aiming at maximizing energy efficiency, the corresponding system throughput saturates in the high transmit power allowance regime, i.e.,  $P_T \geq 37$  dBm. In fact, the energy-efficient SUDAS does not further increase the DL transmit power since the system throughput gain due to a higher transmit power cannot compensate for the increased transmit power, i.e., the energy efficiency would decrease. As for the benchmark and baseline systems aiming at system throughput maximization, the average system throughput increases with the DL transmit power without saturation. For system throughput maximization, the BS always utilizes the entire available DL power budget. Yet, the increased system throughput comes at the expense of a severely degraded system energy efficiency, cf. Figure 4.

#### D. Average System Performance versus Number of SUDACs

Figures 7 and 8 illustrate the average energy efficiency and throughput versus the number of SUDACs for  $N = 8$  BS antennas,  $P_T = 37$  dBm, and different systems. It can be observed that both the system energy efficiency and the system throughput of the proposed SUDAS grow with the number of SUDACs, despite the increased power consumption associated with each additional SUDAC. For  $N \geq M$ , for DL transmission, additional SUDACs facilitate a more efficient conversion of the spatial multiplexing gain in the licensed band to a frequency multiplexing gain in the unlicensed band which leads to a significant data rate improvement. Similarly, for UL transmission, the SUDACs help in converting the frequency multiplexing gain in the unlicensed band to a spatial multiplexing gain in the licensed band. For  $M > N$ , increasing the number of SUDACs in the system leads to more spatial diversity which also improves energy efficiency and system throughput. Besides, a substantial performance gain can be achieved by the SUDAS compared to the baseline system for an increasing number of available SUDACs.

## VI. CONCLUSIONS

In this paper, we studied the resource allocation algorithm design for SUDAS assisted outdoor-to-indoor communication. Specifically, the proposed SUDAS simultaneously utilizes licensed and unlicensed frequency bands to facilitate spatial and frequency multiplexing gains for single-antenna UEs in DL and UL, respectively. The resource allocation algorithm design was formulated as a non-convex matrix optimization problem. In order to obtain a tractable solution, we revealed the structure of the optimal precoding matrices such that the problem could be transformed into a scalar optimization problem. Based on this result, we proposed an asymptotically globally optimal and a suboptimal iterative resource allocation algorithm to solve the problem by alternating optimization. Our simulation results showed that the proposed SUDAS assisted transmission provides substantial energy efficiency and throughput gains

compared to baseline systems which utilize only the licensed frequency spectrum for communication.

#### APPENDIX-PROOF OF THEOREM 2

Due to the page limitation, we provide only a sketch of the proof which follows a similar approach as in [24], [25] and uses majorization theory. We show that the optimal precoding and post-processing matrices jointly diagonalize the DL and UL end-to-end channel matrices on each subcarrier for the maximization of the transformed objective function in subtractive form in (27). First, we consider the objective function in subtractive form for UE  $k$  on a per-subcarrier basis with respect to the optimization variables. In particular, the per-subcarrier objective function for UE  $k$  consists of two parts,

$$\begin{aligned} f_1(\mathcal{P}, \mathcal{S}) &= -s_{\text{DL}}^{[i,k]} \log_2 \left( \det[\mathbf{E}_{\text{DL}}^{[i,k]}] \right) - s_{\text{UL}}^{[i,k]} \log_2 \left( \det[\mathbf{E}_{\text{UL}}^{[i,k]}] \right), \\ f_2(\mathcal{P}, \mathcal{S}) &= s_{\text{DL}}^{[i,k]} \varepsilon_{\text{B}} \text{Tr} \left( \mathbf{P}_{\text{DL}}^{[i,k]} (\mathbf{P}_{\text{DL}}^{[i,k]})^H \right) + s_{\text{DL}}^{[i,k]} \varepsilon_{\text{S}} \text{Tr} \left( \mathbf{G}_{\text{DL}}^{[i,k]} \right) \\ &\quad + s_{\text{UL}}^{[i,k]} \varepsilon_{\text{S}} \text{Tr} \left( \mathbf{G}_{\text{UL}}^{[i,k]} \right) + \varepsilon_k s_{\text{UL}}^{[i,k]} \text{Tr} \left( \mathbf{P}_{\text{UL}}^{[i,k]} (\mathbf{P}_{\text{UL}}^{[i,k]})^H \right), \end{aligned} \quad (74)$$

such that the maximization of the per subcarrier objective function can be expressed as

$$\underset{\mathcal{P}, \mathcal{S}}{\text{minimize}} -f_1(\mathcal{P}, \mathcal{S}) + \eta_{\text{eff}} f_2(\mathcal{P}, \mathcal{S}). \quad (75)$$

Besides, the determinant of the MSE matrix on subcarrier  $i$  for UE  $k$  can be written as

$$\det \left( \mathbf{E}_{\text{DL}}^{[i,k]} \right) = \prod_{j=1}^{N_{\text{S}}} \left[ \mathbf{E}_{\text{DL}}^{[i,k]} \right]_{j,j}, \quad (76)$$

where  $[\mathbf{X}]_{a,b}$  extracts the  $(a,b)$ -th element of matrix  $\mathbf{X}$ .  $f_1(\mathcal{P}, \mathcal{S})$  is a Schur-concave function with respect to the optimal precoding matrices [24] for a given subcarrier allocation policy  $\mathcal{S}$ . Thus,  $-f_1(\mathcal{P}, \mathcal{S})$  is minimized when the MSE matrix  $\mathbf{E}_{\text{DL}}^{[i,k]}$  is a diagonal matrix. Furthermore, the trace operator in  $f_2(\mathcal{P}, \mathcal{S})$  for the computation of the total power consumption is also a Schur-concave function with respect to the optimal precoding matrices. Thus, the optimal precoding matrices for the minimization of function  $f_2(\mathcal{P}, \mathcal{S})$  should diagonalize the input matrix of the trace function, cf. [43, Chapter 9.B.1] and [43, Chapter 9.H.1.h]. Similarly, the power consumption functions on the left hand side of constraints C1–C4 in (27) are also Schur-concave functions and are minimized if the input matrices of the trace functions are diagonal. Besides, the non-negative weighted sum of Schur-concave functions over the subcarrier and UE indices preserves Schur-concavity. In other words, the optimal precoding matrices should jointly diagonalize the subtractive form objective function in (27) and simultaneously diagonalize matrices  $\mathbf{P}_{\text{UL}}^{[i,k]} (\mathbf{P}_{\text{UL}}^{[i,k]})^H$ ,  $\mathbf{P}_{\text{DL}}^{[i,k]} (\mathbf{P}_{\text{DL}}^{[i,k]})^H$ ,  $\mathbf{G}_{\text{UL}}^{[i,k]}$ , and  $\mathbf{G}_{\text{DL}}^{[i,k]}$ . This observation establishes a necessary condition for the structure of the optimal precoding matrices. Finally, by performing SVD on the channel matrices and after some mathematical manipulations, it can be verified that the matrices in (30) and (32) satisfy the optimality condition.

#### REFERENCES

- [1] M. Breiling, D. W. K. Ng, C. Rohde, F. Burkhardt, and R. Schober, "Resource Allocation for Outdoor-to-Indoor Multicarrier Transmission with Shared UE-side Distributed Antenna Systems," in *Proc. IEEE Veh. Techn. Conf.*, May 2015.
- [2] E. Larsson, O. Edfors, F. Tufvesson, and T. Marzetta, "Massive MIMO for Next Generation Wireless Systems," *IEEE Commun. Mag.*, vol. 52, pp. 186–195, Feb. 2014.
- [3] D. Ng, E. Lo, and R. Schober, "Energy-Efficient Resource Allocation in OFDMA Systems with Large Numbers of Base Station Antennas," *IEEE Trans. Wireless Commun.*, vol. 11, pp. 3292–3304, Sep. 2012.
- [4] A. Swindlehurst, E. Ayanoglu, P. Heydari, and F. Capolino, "Millimeter-Wave Massive MIMO: The Next Wireless Revolution?" *IEEE Commun. Mag.*, vol. 52, pp. 56–62, Sep. 2014.
- [5] F. Boccardi, R. Heath, A. Lozano, T. Marzetta, and P. Popovski, "Five Disruptive Technology Directions for 5G," *IEEE Commun. Mag.*, vol. 52, pp. 74–80, Feb. 2014.
- [6] T. Rappaport, S. Sun, R. Mayzus, H. Zhao, Y. Azar, K. Wang, G. Wong, J. Schulz, M. Samimi, and F. Gutierrez, "Millimeter Wave Mobile Communications for 5G Cellular: It Will Work!" *IEEE Access*, vol. 1, pp. 335–349, 2013.
- [7] H. Xu, V. Kukshya, and T. Rappaport, "Spatial and Temporal Characteristics of 60-GHz Indoor Channels," *IEEE J. Select. Areas Commun.*, vol. 20, pp. 620–630, Apr. 2002.
- [8] (2013) Ericsson Mobility Report. [Online]. Available: <http://ec.europa.eu/digital-agenda/en/news/2014-report-implementation-eu-regulatory-framework-electronic-communications>
- [9] R. Heath, S. Peters, Y. Wang, and J. Zhang, "A Current Perspective on Distributed Antenna Systems for the Downlink of Cellular Systems," *IEEE Commun. Mag.*, vol. 51, pp. 161–167, Apr. 2013.
- [10] H. Zhu, "On Frequency Reuse in Cooperative Distributed Antenna Systems," *IEEE Commun. Mag.*, no. 4, pp. 85–89, Apr. 2012.
- [11] R. W. Heath, "What is the Role of MIMO in Future Cellular Networks: Massive? Coordinated? mmWave?" *Presentation delivered at Int. Conf. on Commun.*, Jun. 2013. [Online]. Available: [http://users.ece.utexas.edu/~rheath/presentations/2013/Future\\_of\\_MIMO\\_Plenary\\_Heath.pdf](http://users.ece.utexas.edu/~rheath/presentations/2013/Future_of_MIMO_Plenary_Heath.pdf)
- [12] M. Dohler, "Virtual Antenna Arrays," Ph.D. dissertation, King's College London, University of London, Nov. 2003.
- [13] T. Maciel and A. Klein, "On the Performance, Complexity, and Fairness of Suboptimal Resource Allocation for Multiuser MIMO-OFDMA Systems," *IEEE Trans. Veh. Technol.*, vol. 59, pp. 406–419, Jan. 2010.
- [14] C.-M. Yen, C.-J. Chang, and L.-C. Wang, "A Utility-Based TMCR Scheduling Scheme for Downlink Multiuser MIMO-OFDMA Systems," *IEEE Trans. Veh. Technol.*, vol. 59, pp. 4105–4115, Oct. 2010.
- [15] H. Zhu and J. Wang, "Resource Allocation in OFDMA-Based Distributed Antenna Systems," in *Proc. IEEE/CIC IEEE Intern. Commun. Conf. in China*, Aug 2013, pp. 565–570.
- [16] CISCO: The Internet of Things. [Online]. Available: <http://share.cisco.com/internet-of-things.html>
- [17] J. Jiang, M. Dianati, M. Imran, and Y. Chen, "Energy Efficiency and Optimal Power Allocation in Virtual-MIMO Systems," in *Proc. IEEE Veh. Techn. Conf.*, Sep. 2012.
- [18] C. He, B. Sheng, P. Zhu, X. You, and G. Li, "Energy- and Spectral-Efficiency Tradeoff for Distributed Antenna Systems with Proportional Fairness," *IEEE J. Select. Areas Commun.*, vol. 31, pp. 894–902, May 2013.
- [19] X. Chen, X. Xu, and X. Tao, "Energy Efficient Power Allocation in Generalized Distributed Antenna System," *IEEE Commun. Lett.*, vol. 16, pp. 1022–1025, Jul. 2012.
- [20] SUDAS - UE-Side Virtual MIMO using MM-Wave for 5G. [Online]. Available: [www.iis.fraunhofer.de/sudas](http://www.iis.fraunhofer.de/sudas)
- [21] J. Andrews, "Seven Ways that HetNets are a Cellular Paradigm Shift," *IEEE Commun. Mag.*, vol. 51, pp. 136–144, Mar. 2013.
- [22] D. W. K. Ng, E. S. Lo, and R. Schober, "Energy-Efficient Resource Allocation in Multi-Cell OFDMA Systems with Limited Backhaul Capacity," *IEEE Trans. Wireless Commun.*, vol. 11, pp. 3618–3631, Oct. 2012.
- [23] M. Breiling, D. W. K. Ng, C. Rohde, F. Burkhardt, R. Schober, and T. Heyn, "UE-Side Virtual MIMO Using MM-Wave For 5G," Fraunhofer-Institute For Integrated Circuits (IIS), Erlangen/Germany; Friedrich-Alexander University Erlangen-Nürnberg, Germany, Tech. Rep., Aug. 2014. [Online]. Available: [http://www.iis.fraunhofer.de/content/dam/iis/en/doc/ks/bb/SUDAS\\_Whitepaper.pdf](http://www.iis.fraunhofer.de/content/dam/iis/en/doc/ks/bb/SUDAS_Whitepaper.pdf)
- [24] Y. Rong, X. Tang, and Y. Hua, "A Unified Framework for Optimizing Linear Nonregenerative Multicarrier MIMO Relay Communication

- Systems," *IEEE Trans. Signal Process.*, vol. 57, pp. 4837 – 4851, Dec. 2009.
- [25] D. W. K. Ng, E. S. Lo, and R. Schober, "Dynamic Resource Allocation in MIMO-OFDMA Systems with Full-Duplex and Hybrid Relaying," *IEEE Trans. Commun.*, vol. 60, pp. 1291–1304, May 2012.
- [26] D. W. K. Ng and R. Schober, "Cross-Layer Scheduling for OFDMA Amplify-and-Forward Relay Networks," *IEEE Trans. Veh. Technol.*, vol. 59, pp. 1443–1458, Mar. 2010.
- [27] I. Hammerstrom and A. Wittneben, "Power Allocation Schemes for Amplify-and-Forward MIMO-OFDM Relay Links," *IEEE Trans. Wireless Commun.*, vol. 6, pp. 2798–2802, Aug. 2007.
- [28] W. Dinkelbach, "On Nonlinear Fractional Programming," *Management Science*, vol. 13, pp. 492–498, Mar. 1967. [Online]. Available: <http://www.jstor.org/stable/2627691>
- [29] D. Ng, E. Lo, and R. Schober, "Energy-Efficient Resource Allocation for Secure OFDMA Systems," *IEEE Trans. Veh. Technol.*, vol. 61, pp. 2572–2585, Jul. 2012.
- [30] W. Yu and R. Lui, "Dual Methods for Nonconvex Spectrum Optimization of Multicarrier Systems," *IEEE Trans. Commun.*, vol. 54, pp. 1310 – 1321, Jul. 2006.
- [31] K. Seong, M. Mohseni, and J. Cioffi, "Optimal Resource Allocation for OFDMA Downlink Systems," in *Proc. IEEE Intern. Sympos. on Inf. Theory*, Jul. 2006, pp. 1394–1398.
- [32] S. Boyd and L. Vandenberghe, *Convex Optimization*. Cambridge University Press, 2004.
- [33] J. C. Bezdek and R. J. Hathaway, "Convergence of Alternating Optimization," *Neural, Parallel and Sci. Comput.*, vol. 11, pp. 351–368, Dec. 2003.
- [34] N. Papandreou and T. Antonakopoulos, "Bit and Power Allocation in Constrained Multicarrier Systems: The Single-user Case," *EURASIP J. Adv. Signal Process.*, vol. 2008, Jan. 2008.
- [35] M. T. Heath, *Scientific Computing: An Introductory Survey*. McGraw-Hill, 2015.
- [36] T. H. Cormen, C. E. Leiserson, R. L. Rivest, and C. Stein, *Introduction to Algorithms*, 3rd ed. The MIT Press, 2009.
- [37] J. Meiniälä, P. Kyösti, L. Hentilä, T. Jämsä, E. K. Essi Suikkanen, and M. Narandžić, "Wireless World Initiative New Radio WINNER+, D5.3: WINNER+ Final Channel Models," CELTIC Telecommunication Solutions, Tech. Rep.
- [38] "Technical Specification Group Radio Access Network; Evolved Universal Terrestrial Radio Access (E-UTRA); Physical Channels and Modulation (Release 8)," 3rd Generation Partnership Project, Tech. Rep., 3GPP, TS 36.211, V8.9.0.
- [39] A. Maltsev, V. Erceg, E. Perahia, C. Hansen, R. Maslennikov, A. Lomayev, A. Sevastyanov, A. Khoryaev, G. Morozov, M. Jacob, T. K. S. Priebe, S. Kato, H. Sawada, K. Sato, and H. Harada, "Channel Models for 60 GHz WLAN Systems," IEEE Tech. Rep. 802.11-09/0334r8, Tech. Rep.
- [40] O. Arnold, F. Richter, G. Fettweis, and O. Blume, "Power Consumption Modeling of Different Base Station Types in Heterogeneous Cellular Networks," in *Proc. Future Network and Mobile Summit*, 2010, pp. 1–8.
- [41] R. Kumar and J. Gurugubelli, "How Green the LTE Technology Can be?" in *Intern. Conf. on Wireless Commun., Veh. Techn., Inform. Theory and Aersp. Electron. Syst. Techn.*, Mar. 2011.
- [42] M. Miyahara, H. Sakaguchi, N. Shimasaki, and A. Matsuzawa, "An 84 mW 0.36 mm<sup>2</sup> Analog Baseband Circuits For 60 GHz Wireless Transceiver in 40 nm CMOS," in *Proc. IEEE Radio Freq. Integr. Circuits Sympos. (RFIC)*, Jun. 2012, pp. 495–498.
- [43] A. W. Marshall and I. Olkin, *Inequalities: Theory of Majorization and its Applications*. New York: Academic Press, 1979.



**Derrick Wing Kwan Ng (S'06-M'12)** received the bachelor degree with first class honors and the Master of Philosophy (M.Phil.) degree in electronic engineering from the Hong Kong University of Science and Technology (HKUST) in 2006 and 2008, respectively. He received his Ph.D. degree from the University of British Columbia (UBC) in 2012. In the summer of 2011 and spring of 2012, he was a visiting scholar at the Centre Tecnològic de Telecomunicacions de Catalunya - Hong Kong (CTTC-HK). He was a senior postdoctoral fellow at the Institute for Digital Communications, Friedrich-Alexander-University Erlangen-Nürnberg (FAU), Germany. He is now working as a Lecturer at the University of New South Wales, Sydney, Australia. His research interests include convex and non-convex optimization, physical layer security, wireless information and power transfer, and green (energy-efficient) wireless communications.

Dr. Ng received the Best Paper Awards at the IEEE Wireless Communications and Networking Conference (WCNC) 2012, the IEEE Global Telecommunication Conference (Globecom) 2011, and the IEEE Third International Conference on Communications and Networking in China 2008. He was awarded the IEEE Student Travel Grants for attending the IEEE WCNC 2010, the IEEE International Conference on Communications (ICC) 2011, and the IEEE Globecom 2011. He was also the recipient of the 2009 Four Year Doctoral Fellowship from the UBC, Sumida & Ichiro Yawata Foundation Scholarship in 2008, and R&D Excellence Scholarship from the Center for Wireless Information Technology in HKUST in 2006. He has served as an editorial assistant to the Editor-in-Chief of the IEEE Transactions on Communications since Jan. 2012. He is currently an Editor of the IEEE Communications Letters. He was a Co-Chair for the Wireless Access Track of 2014 IEEE 80th Vehicular Technology Conference. He has been a TPC member of various conferences, including the Globecom, WCNC, ICC, VTC, and PIMRC, etc. He was honoured as the top reviewer of the IEEE Transactions on Vehicular Technology in 2014 and an Exemplary Reviewer of the IEEE Wireless Communications Letters for 2012, 2014.



**Marco Breiling** was born in Birkenfeld/Nahe, Germany, in 1970. After conducting studies at the Universität Karlsruhe/Germany (now Karlsruhe Institute of Technology KIT), the Norges Tekniske Høgskole (NTH) in Trondheim/Norway (now Norges Teknisk-Naturvitenskapelige Universitet NTNU), the Ecole Supérieure d'Ingénieurs en Electronique et Electrotechnique (ESIEE) in Paris, and the University of Southampton/England, he graduated with a Dipl.-Ing. (equivalent to master's) degree from KIT in 1997. He earned his PhD degree (with highest

honors) for a thesis about turbo codes from Friedrich-Alexander-University Erlangen-Nürnberg (FAU), Germany in 2002. Since 2001, he has been working at the Fraunhofer Institute for Integrated Circuits (IIS) in Erlangen in the field of digital communications. His special interests are channel coding, iterative processing and virtual MIMO. He currently holds the chief scientist position of the broadband & broadcast department. Moreover, he is a Distinguished Lecturer of the IEEE Broadcast Technology Society.



**Christian Rohde** was born in Erlangen, Germany, in 1979. He received his Diplom degree (Dipl.-Ing.) and his PhD degree (Dr.-Ing.) in electrical engineering from the Chair of Mobile Communications of the Friedrich-Alexander-University Erlangen-Nürnberg (FAU), Germany, in 2005 and 2013, respectively. Since his graduation, he is with the Communication Systems Division of the Fraunhofer Institute for Integrated Circuits IIS as a senior research engineer. His research and development interests include physical layer system design and algorithms

for receiver synchronization for both, single-carrier and multi-carrier transmission. Special focus is on adaptive channel estimation and equalization algorithms, which are robust against severe channel or interference conditions and are of relevance for implementation. Since 2012, he is active member of the technical module for satellite communications (TM-S) of the Digital Video Broadcasting Project (DVB) and has contributed to the standardization of DVB-S2X.



**Frank Burkhardt** was born in Erlangen, Germany, in 1972. He received his Diplom degree (Dipl.-Ing.) in electrical engineering at the of the Friedrich-Alexander-University Erlangen-Nürnberg (FAU), Germany, in 2001. Since his graduation, he is with the Communication Systems Division of the Fraunhofer Institute for Integrated Circuits IIS as a senior research engineer. His research and development interests include design and implementation of software defined radio systems (SDR) and modeling of radio propagation channels.



**Robert Schober (M'01, SM'08, F'10)** was born in Neuendettelsau, Germany, in 1971. He received the Diplom (Univ.) and the Ph.D. degrees in electrical engineering from the University of Erlangen-Nürnberg in 1997 and 2000, respectively. From May 2001 to April 2002 he was a Postdoctoral Fellow at the University of Toronto, Canada, sponsored by the German Academic Exchange Service (DAAD). Since May 2002 he has been with the University of British Columbia (UBC), Vancouver, Canada, where he is now a Full Professor. Since

January 2012 he is an Alexander von Humboldt Professor and the Chair for Digital Communication at the Friedrich Alexander University (FAU), Erlangen, Germany. His research interests fall into the broad areas of Communication Theory, Wireless Communications, and Statistical Signal Processing.

Dr. Schober received the 2002 Heinz MaierLeibnitz Award of the German Science Foundation (DFG), the 2004 Innovations Award of the Vodafone Foundation for Research in Mobile Communications, the 2006 UBC Killam Research Prize, the 2007 Wilhelm Friedrich Bessel Research Award of the Alexander von Humboldt Foundation, the 2008 Charles McDowell Award for Excellence in Research from UBC, a 2011 Alexander von Humboldt Professorship, and a 2012 NSERC E.W.R. Steacie Fellowship. In addition, he received best paper awards from the German Information Technology Society (ITG), the European Association for Signal, Speech and Image Processing (EURASIP), IEEE WCNC 2012, IEEE Globecom 2011, IEEE ICUWB 2006, the International Zurich Seminar on Broadband Communications, and European Wireless 2000. Dr. Schober is a Fellow of the Canadian Academy of Engineering and a Fellow of the Engineering Institute of Canada. He is currently the Editor-in-Chief of the IEEE Transactions on Communications.